DOI:10.14753/SE.2022.2632

BICARBONATE INHIBITS THE GROWTH AND BIOFILM FORMATION OF PATHOGENS RELEVANT TO CYSTIC FIBROSIS

Ph.D. Doctoral Dissertation

Pongsiri Jaikumpun

Doctoral School of Clinical Medicine

Semmelweis University

Supervisors:
Dr. Ákos Zsembery, M.D., Ph.D.
Dr. Orsolya Dobay, Ph.D.

Official reviewers:
Dr. Levente Karaffa, Ph.D., D.Sc.
Dr. László Kőhidai, CSc, Ph.D.

Head of the Complex Examination Committee:
Dr. József Barabás, Ph.D.

Members of the Complex Examination Committee:
Prof. Dr. István Gera, CSc, Ph.D.
Prof. Dr. Zoltán Rakonczay, CSc, D.Sc.

Budapest

2021

DOI:10.14753/SE.2022.2632

Table of Contents

DOI:10.14753/SE.2022.2632

DOI:10.14753/SE.2022.2632

DOI:10.14753/SE.2022.2632

List of Abbreviations

ABC	ATP-binding cassette protein channels superfamily
AE2	Cl^-/HCO_3^- Exchanger
ASM	Artificial sputum medium
ASL	Airway surface liquid
AMPs	Antimicrobial peptides
ANO1	Ca^{2+} activated Cl^- channel
ANOVA	Analysis of variance
ATCC®	American Type Culture Collection
ATP	Adenosine triphosphate
ATP12A	ATPase H^+/K^+ transporting non-gastric alpha2 subunit
AUC	Area under the curve
*Bac*Light	LIVE/DEAD *Bac*Light Bacteria Viability Kit
BHI	Brian-heart infusion medium
BSA	Bovine serum albumin
CA	Carbonic anhydrase enzyme
cAMP	Cyclic adenosine monophosphate
CBF	Cilia beating frequency
CCL20	Chemokine ligand 20 or Macrophage Inflammatory Protein-3
CF	Cystic fibrosis

DOI:10.14753/SE.2022.2632

CFC	Cystic Fibrosis Canada
CFF	Cystic Fibrosis Foundation
CFFA	Cystic Fibrosis Federation Australia
CFTR	Cystic fibrosis transmembrane conductance regulator
CFU	Colony-forming unit assay
COPD	Chronic obstructive pulmonary diseases
CV	Crystal violet
CVA	Crystal violet assay
DNA	Deoxyribonucleic acid
DTPA	Diethylenetriaminepentaacetic acid
ECFS	European Cystic Fibrosis Society
EDTA	Ethylenediaminetetraacetic acid
ENaC	Epithelial sodium channel
ep	Epithelium
FC	Flow cytometry
FL1, FL3	Specific fluorescence intensity
FSC	Forward scatter
F508del	CFTR mutation causing the loss of a phenylalanine at the 508th position
ΔF508	CFTR mutation causing the loss of a phenylalanine at the 508th position
ΔF508-CFTR CFBE	Mutant (ΔF508) human bronchial epithelial cells

DOI:10.14753/SE.2022.2632

GBEFC	Brazilian Cystic Fibrosis Study Group
HVCN1	Hydrogen voltage-gated channel 1
IV	Intravenous
L	Lumen
lp	Lamina propria
LSD	Fisher's Least Significant Difference test
MCC	Mucociliary clearance
MCL	Mucus layer
MCT	Mucociliary transport
MUC	Mucin or mucin gene
NADs	Nucleic acid double staining
NBCe1	Electrogenic Na-coupled bicarbonate co-transporter 1
NBDs	Nucleotide-binding domains
NHE1	Na^+/H^+ exchanger 1
NKA	Na^+/K^+ ATPase
NKCC	Na^+ K^+ Cl^- cotransporter
NSAIDs	Nonsteroidal anti-inflammatory drugs
OD	Optical density
p	*p*-value of statistical significance
PA	*Pseudomonas aeruginosa*

PCL	Periciliary liquid
Pdn	Pendrin protein transporter
Phe508del	CFTR mutation causing the loss of a phenylalanine at the 508th position
PI	Propidium iodide
PKA	Protein kinase A
PKC	Protein kinase C
PLANC	Palate, lung, and nasal epithelial clone
RD	Regulatory domain
SA	*Staphylococcus aureus*
SD	Standard deviation
SGs	Secretory granules
SSC	Side scatter
TMDs	Transmembrane domains
V-ATPase	Vacuolar-type ATPase
WinCF	Winogradsky-based culture system for CF microbiology
WT-CFTR CFBE	Wild-type CFTR human bronchial epithelial cells

DOI:10.14753/SE.2022.2632

1. Introduction

1.1. Cystic fibrosis

Cystic fibrosis (CF) is a life-limiting genetic disorder caused by mutations in the cystic fibrosis transmembrane conductance regulator (CFTR) gene [1]. This gene encodes the CFTR protein, an epithelial anion channel found throughout the body, especially in the respiratory and gastrointestinal tracts. CFTR channel primarily transports chloride (Cl^-) and bicarbonate (HCO_3^-) ions [2-4] and regulates sodium ion (Na^+) absorption via the epithelial sodium channels (ENaCs) [5], which are very important for fluid balance across the epithelial cell layers.

Mutations in the CFTR gene result in protein dysfunction, disrupting transepithelial electrolyte and water movements in many organs. The most affected organs are the lungs and pancreas. However, chronic lung disease and pulmonary exacerbation due to bacterial infection are the leading cause of death in CF.

1.1.1. Epidemiology

CF is inherited primarily in the Caucasian population. It affects around one in 2,500 to 3,500 white newborns, whereas the incidence is very low for African American and Asian American newborns, which are approximately one in 17,000 and 31,000 babies, respectively [6]. It is estimated that currently, there are approximately 100,000 people worldwide living with CF. In the US, there were 31,199 diagnosed with CF [7], and there were 4,344 cases in Canada [8], 3,446 patients in Australia [9], and 5,417 in Brazil [10]. According to the European Cystic Fibrosis Society (ECFS) report in 2018, there were 49,886 CF patients in Europe, with approximately 498 cases in Hungary [11]. Burgel *et al.* predicted that by 2025 the percentage of CF patients in Europe and Hungary would increase 50% and 60.5%, respectively, because of the overall improvement of the healthcare system [12].

The CF registry records in Asian countries are limited. One reason could be because the incidence of CF in Asia is very low. A recent report reveals that there might be approximately 30 CF cases in Japan, 60 – 100 cases in South Korea, 60 cases in Malaysia, 95 cases in Bangladesh, 40 cases in Thailand, 18 cases in Singapore, and 12

cases in Taiwan [13]. However, these numbers are estimated by the healthcare workers in the countries. The actual numbers are still unknown because a comprehensive data collection is currently not available.

1.1.2. Life expectancy

Before the 20th century, CF was known as a mysterious disease that killed small children in their early life [14]. In the 21st century, due to our better understanding of the disease and improvement of the healthcare system, the overall trend of median age of death and survival of CF patients have significantly increased, although data vary among regions.

The median predicted survival age of CF babies born in 2019 was 48.4 years in the US, while the median age at death was 32.4 years (Figure 1) [7]. In Australia, the median age of deaths in 2019 was 32 years, while the median age of survival was 53 years for people with CF born in 2015-2019 [9]. In Europe, the median age of the deaths and survival have not been precisely identified. The 2018 European Cystic Fibrosis Society (ECFS) report showed that the most frequent age range at death is 21-30 years [11]. In Canada, the median age of death was 42.1, and the median age of survival was 54.3 years [8], which were the highest numbers ever reported. These numbers represent our better understanding of the disease and the improvement of healthcare management in the last decades.

However, although the median age of death and survival have been continuously increasing each year, the incidence of pulmonary exacerbation and respiratory failure remains high [15, 16]. CFF reported that 41% of CF adults and 22% of children with CF were hospitalized with intravenous (IV) antibiotics due to pulmonary exacerbation in 2019 [17]. This incidence does not seem to be much improved when compared to the older records in 2016 (42% adults and 26% children) [18] and 2017 (43% adults and 24% children) [19], even compared to the records since 2005 (Figure 2 A) [7]. In fact, the annual records of CF patients receiving a lung transplant in the USA (1992 – 2019) uncover that the number of CF patients receiving the lung transplant has been incredibly increasing (Figure 2 B) [7].

DOI:10.14753/SE.2022.2632

This evidence implies that CF lung infection is a significant threat for CF patients. A better understanding of CF-related infectious airway diseases would contribute to developing new therapeutic approaches for the patients.

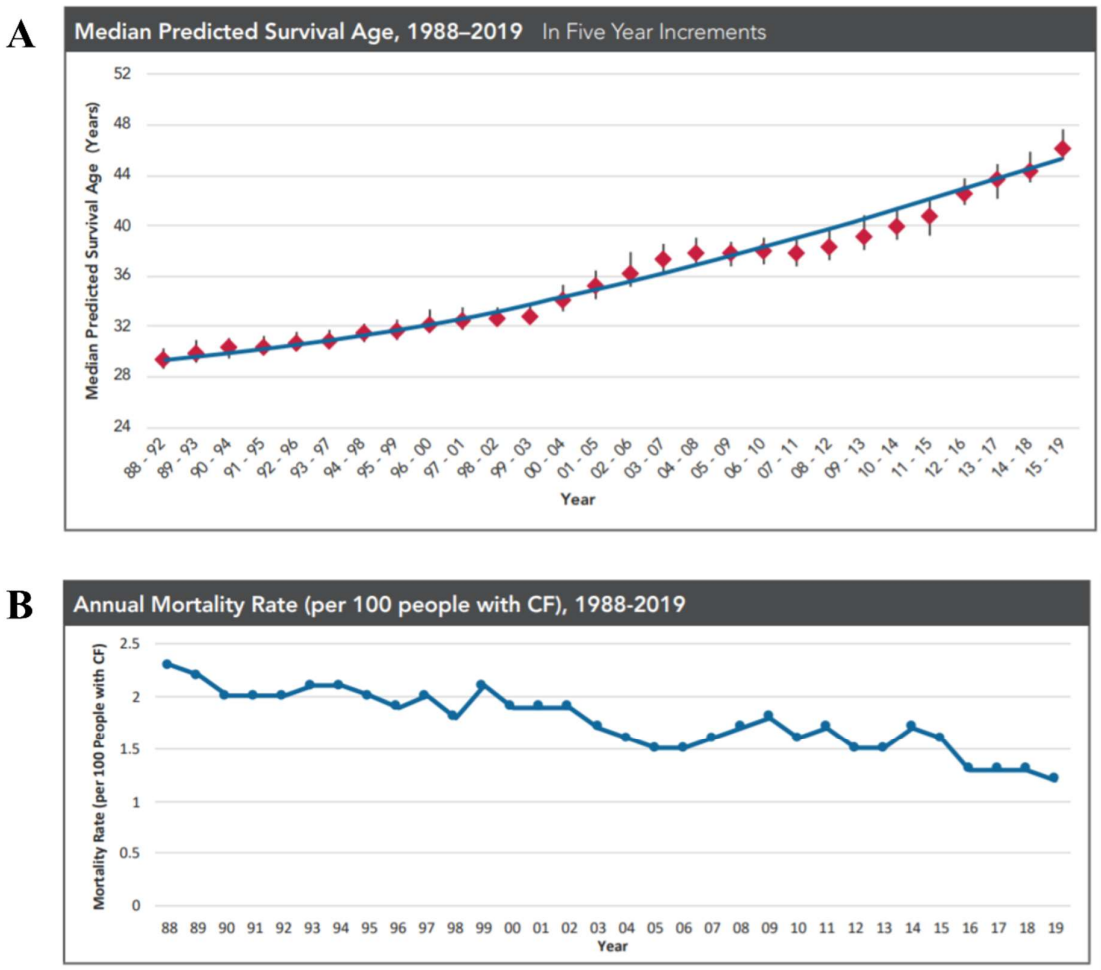

Figure 1. Overall trend of CF survival age and mortality rate in the USA.

(A) Median predicted survival age of CF patients, 1988 – 2019. **(B)** Annual mortality rate of CF patients, 1988 - 2019. The figure was reproduced with permissions from Cystic Fibrosis Foundation Patient Registry: 2019 Annual Data Report, Bethesda, Maryland ©2020 Cystic Fibrosis Foundation [7].

DOI:10.14753/SE.2022.2632

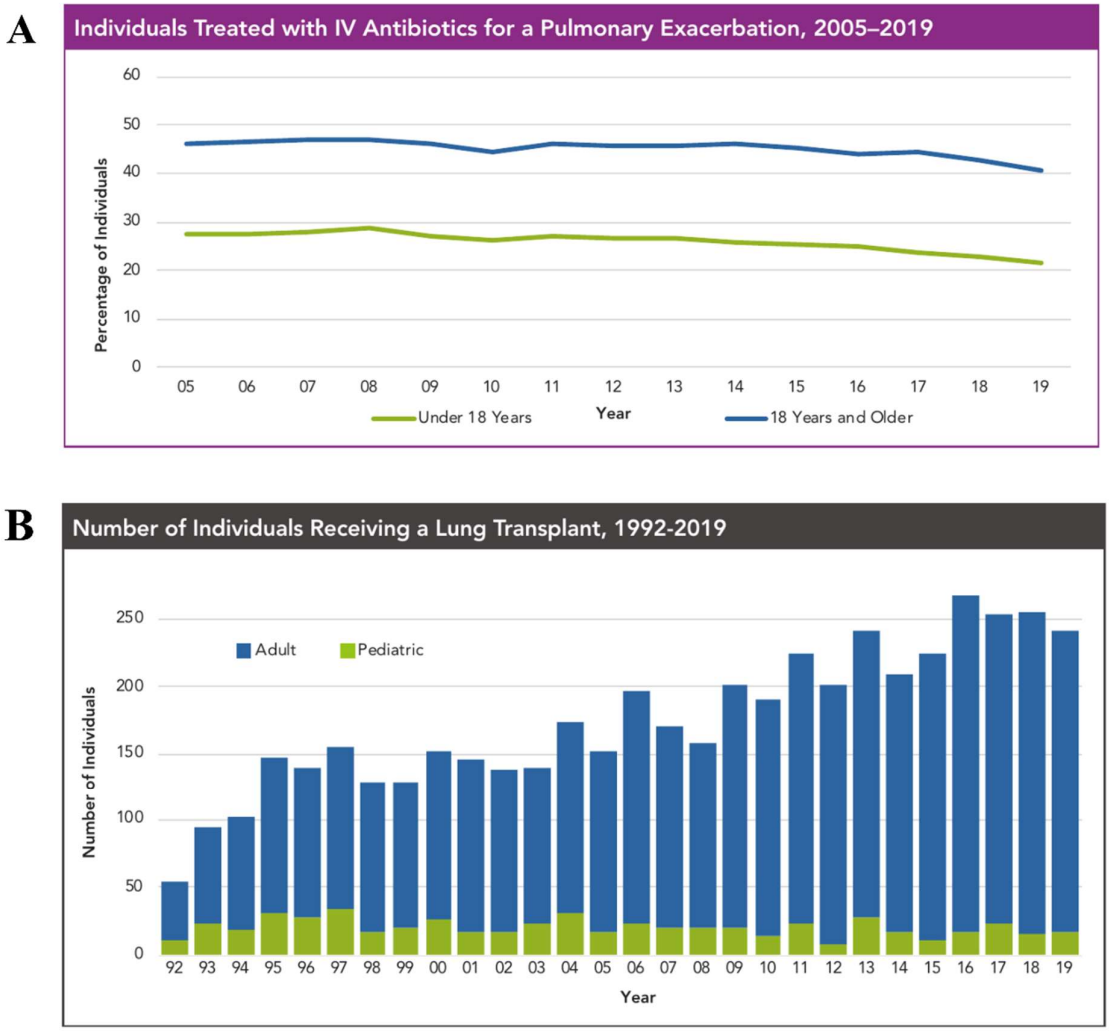

Figure 2. Annual trend of pulmonary exacerbation and lung transplant.

(A) Percentage of individuals treated with IV antibiotics for a pulmonary exacerbation, 2005 – 2019. **(B)** Annual numbers of CF patients in the USA, 1988 - 2019. The figure was reproduced with permissions from Cystic Fibrosis Foundation Patient Registry: 2019 Annual Data Report, Bethesda, Maryland ©2020 Cystic Fibrosis Foundation [7].

1.1.3. Cystic fibrosis and the discovery of CFTR gene

In the 17th century, CF appeared to be an unknown disease described as premature death in children with salty sweat [14]. Until 1938, CF was recognized as a distinct clinical entity and observed by Dorothy H. Andersen [20]. However, the understanding of the disease was very poor at that time.

Lap-Chee Tsui, John R. Riordan, and Francis Collins discovered and identified a gene involved in CF pathology on a single locus of chromosome 7 in 1989. The gene was named "cystic fibrosis transmembrane conductance regulator" or CFTR [1, 21]. Surprisingly, the most common CF mutation, a deletion of three base pairs, which results in the loss of a phenylalanine residue at the position 508 (ΔF508), was also identified in the same year [22].

Both discoveries represent milestones not only in CF research but in general medical sciences as well. Since then, CF has been regarded as a model for genetic diseases, pioneering our understanding of genetics, molecular and cellular mechanisms, and pathogenesis [16]. These historical breakthroughs have also paved the way for the development of therapeutic approaches in other rare genetic disorders and chronic respiratory diseases such as asthma and COPD.

1.1.4. CFTR protein - structure, mechanism, and functions

CFTR is a membrane protein comprising of five domains: two transmembrane domains (TMDs), two cytoplasmic nucleotide-binding domains (NBDs), and one regulatory domain (RD) (Figure 3). The R domain contains phosphorylation sites, responsible for the channel activation, and is structurally located between the two TMD-NBD complexes, interacting with NBD_1, TMD_2, and NBD_2 structures.

When the R domain is dephosphorylated, it prevents the NBD dimerization, thus blocking channel opening. In contrast, in the phosphorylated state, the R domain is stabilized away from the NBD domains, allowing NDB dimerization and conformational changes necessary for channel opening [23, 24].

DOI:10.14753/SE.2022.2632

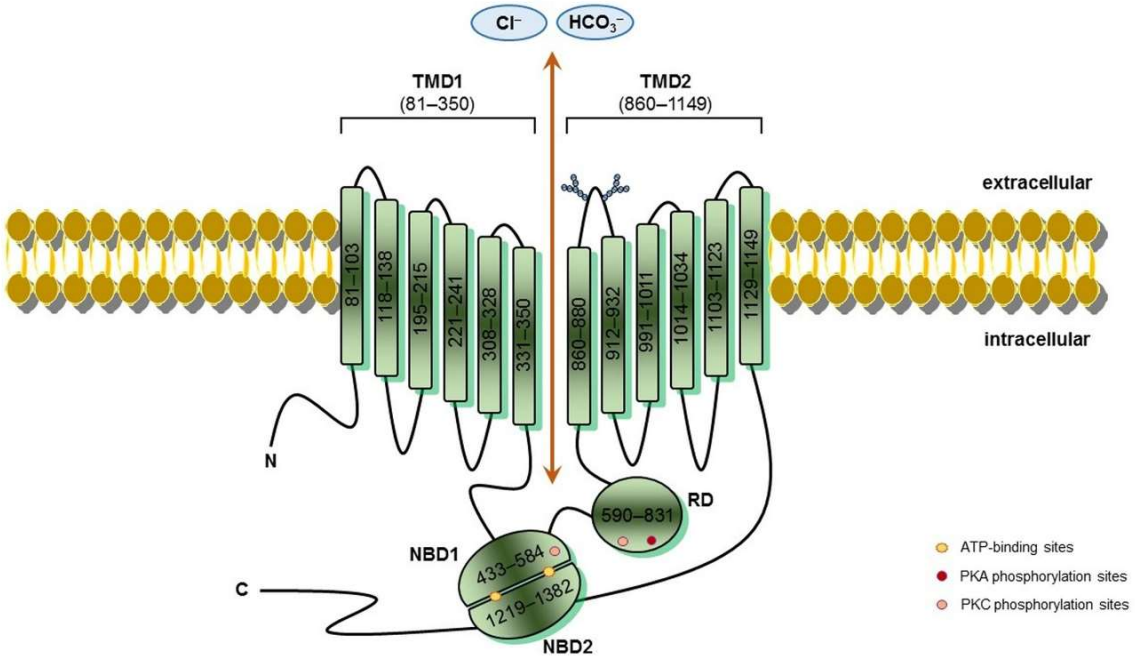

Figure 3. Schematic structure of CFTR.

CFTR consists of five domains: two transmembrane domains (TMD1 and TMD2), two nucleotide-binding domains (NBD1 and NBD2), and one regulatory domain (RD). The figure was reprinted from "CFTR Modulators: Shedding Light on Precision Medicine for Cystic Fibrosis" by M. Lopes-Pacheco, *Front Pharmacol*, (2016) [25].

CFTR is operated by several second messengers, including cyclic AMP (cAMP) dependent protein kinase A (PKA), protein kinase C (PKC), and ATP. Therefore, it is known to belong to the ATP-binding cassette (ABC) transporter superfamily. However, most ABC transporters utilize the chemical energy of ATP hydrolysis to transport substrates against their electrochemical gradient, but CFTR uniquely conducts anions down their electrochemical gradient [26].

CFTR protein is located at the apical surface of epithelial cells. Its primary function is to regulate the transport of anions across epithelial tissues. At the CFTR's pore region, negatively charged molecules such as Cl^- are attracted and accommodated by the positively charged amino acid sidechains. Once the channel is activated, the channel opens, resulting in a rapid movement of Cl^- through the pore [27]. In addition to Cl^-, HCO_3^- has also been reported to pass through the pore [3], and some other organic anions such as thiocyanate ion (SCN^-) can also compete with Cl^- [27].

Furthermore, CFTR also regulates other transport proteins, including ENaC, K^+ channels, ATP-release mechanisms, HCO_3^-/Cl^- exchangers, and aquaporin water channels [28, 29]. These transporters are involved in ion transport regulating transepithelial water movement and luminal pH.

1.1.5. CFTR mutations and protein dysfunction

CF is caused by mutations in the CFTR gene, which lead to either low membrane expression, dysfunctional regulation, or impaired channel function [22]. Until now, more than 2,000 CFTR mutations have been identified [6]. Obviously, different mutations cause different defects. For example, some mutants can induce a reduction in protein expression, whereas some mutants can decrease protein function and stability or combine these malfunctions. These variations result in various clinical manifestations, from milder to more severe symptoms [16]. Researchers have grouped CFTR mutations into seven classes (Figure 4) based on pathological pathways and defects, which are very helpful for developing corrective therapies targeting the specific cause [30, 31].

The most common CFTR mutation belongs to class II mutations, the deletion of phenylalanine in position 508 (ΔF508 or F508del). It accounts for two-thirds of CF cases worldwide and around 90% of cases in the United States [31, 32]. This mutation causes folding defects during protein synthesis. As a result, the protein is prematurely degraded before it can reach the apical pole of the cell, resulting in deficient CFTR expression in the plasma membrane [33, 34].

In many organs, loss of CFTR causes impaired transepithelial electrolyte and water transport across the epithelial cells. The mucus-secreting organs are mainly affected, including the lung, pancreas, liver, intestine, and vas deferens. The only exception is the sweat ducts, which are not involved in mucus secretion. As mentioned above, however, the lung is the most affected organ in CF. Thus, its protection and repair represent the most challenging task for clinicians.

DOI:10.14753/SE.2022.2632

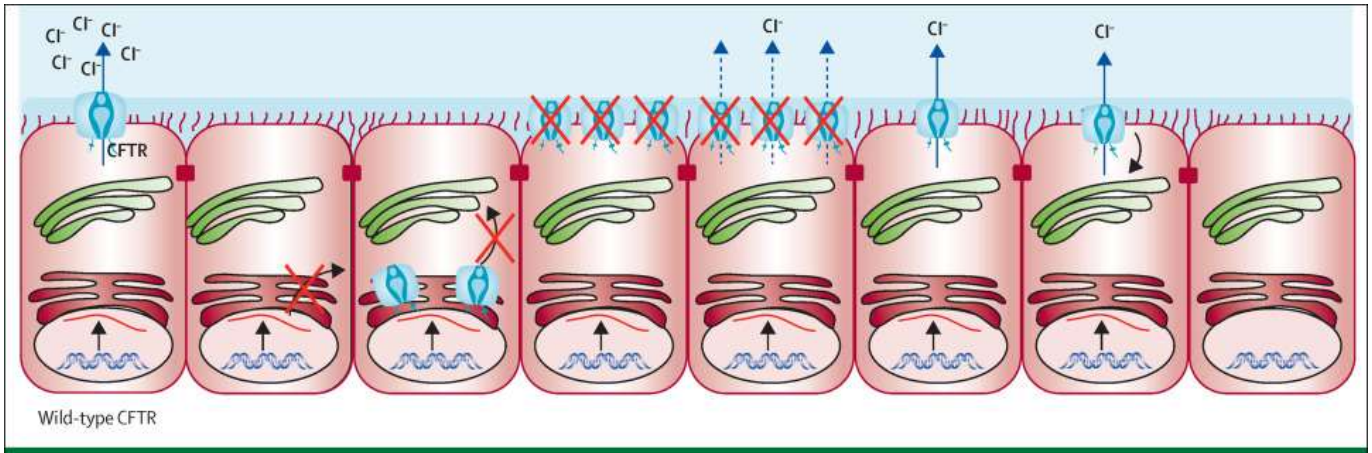

	Class I	Class II	Class III	Class IV	Class V	Class VI	Class VII
CFTR defect	No protein	No traffic	Impaired gating	Decreased conductance	Less protein	Less stable	No mRNA
Mutation examples	Gly542X, Trp1282X	Phe508del, Asn1303Lys, Ala561Glu	Gly551Asp, Ser549Arg, Gly1349Asp	Arg117His, Arg334Trp, Ala455Glu	Ala455Glu, 3272-26A→G, 3849+10 kg C→T	c. 120del23, rPhe508del	dele2,3(21 kb), 1717-1G→A
Corrective therapy	Rescue synthesis	Rescue traffic	Restore channel activity	Restore channel activity	Correct splicing	Promote stability	Unrescuable
Drug (approved)	Read-through compounds (no)	Correctors (yes)	Potentiators (yes)	Potentiators (no)	Antisense oligonucleotides, correctors, potentiators? (no)	Stabilisers (no)	Bypass therapies (no)

Figure 4. Classes of gene mutations and respective therapeutic strategies.

CFTR mutations are grouped into seven functional classes, expecting that the same modulators will apply to all the defects in one class.

The figure was reprinted from “Progress in therapies for cystic fibrosis” by K. De Boeck and M.D. Amaral, *Lancet Respir Med*, (2016) [30].

DOI:10.14753/SE.2022.2632

1.2. Cystic fibrosis lung

1.2.1. Cystic fibrosis lung pathogenesis

CFTR dysfunction causes a decrease in Cl^- and HCO_3^- secretion in the respiratory tract, altering both the volume and composition of the airway surface liquid (ASL). Since CFTR usually controls ENaC, CFTR dysfunction also interferes with ENaC activity, resulting in hyperabsorption of Na^+. As a result, the ASL becomes dehydrated and acidic [35] (Figure 5).

Dehydration and acidification of ASL increase the amount and viscosity of mucus, rendering the mucus more persistent and difficult to remove by the mucociliary clearance (MCC), a cleansing mechanism operated by cilia of airway epithelia sweeping inhaled particles and microbes out of the airways. Therefore, the sticky mucus accumulates and obstructs small airways, leading to chronic airway infections, inflammation, and, consequently, the lung parenchyma's destruction [30, 36].

Indeed, inhaled bacteria cannot be adequately removed from the airways and remain entrapped in the thick mucus, which is the ideal habitat for bacterial growth and colonization [37]. It is noteworthy that CF mucus/sputum is rich in nutrients, optimal temperature, and a slightly acidic pH [35]. Furthermore, the activities of antimicrobial peptides are also compromised due to the acidic airway pH [36, 38].

Due to these environmental changes in CF airways, bacterial colonization occurs with increased risk, leading to chronic respiratory infections. Subsequently, the accumulation of inflammatory mediators and immune cells triggers more aggressive inflammation. This vicious cycle results in lung tissue destruction, remodeling, and scar formation [30, 39], leading to respiratory insufficiency and eventually to the death of the patients.

DOI:10.14753/SE.2022.2632

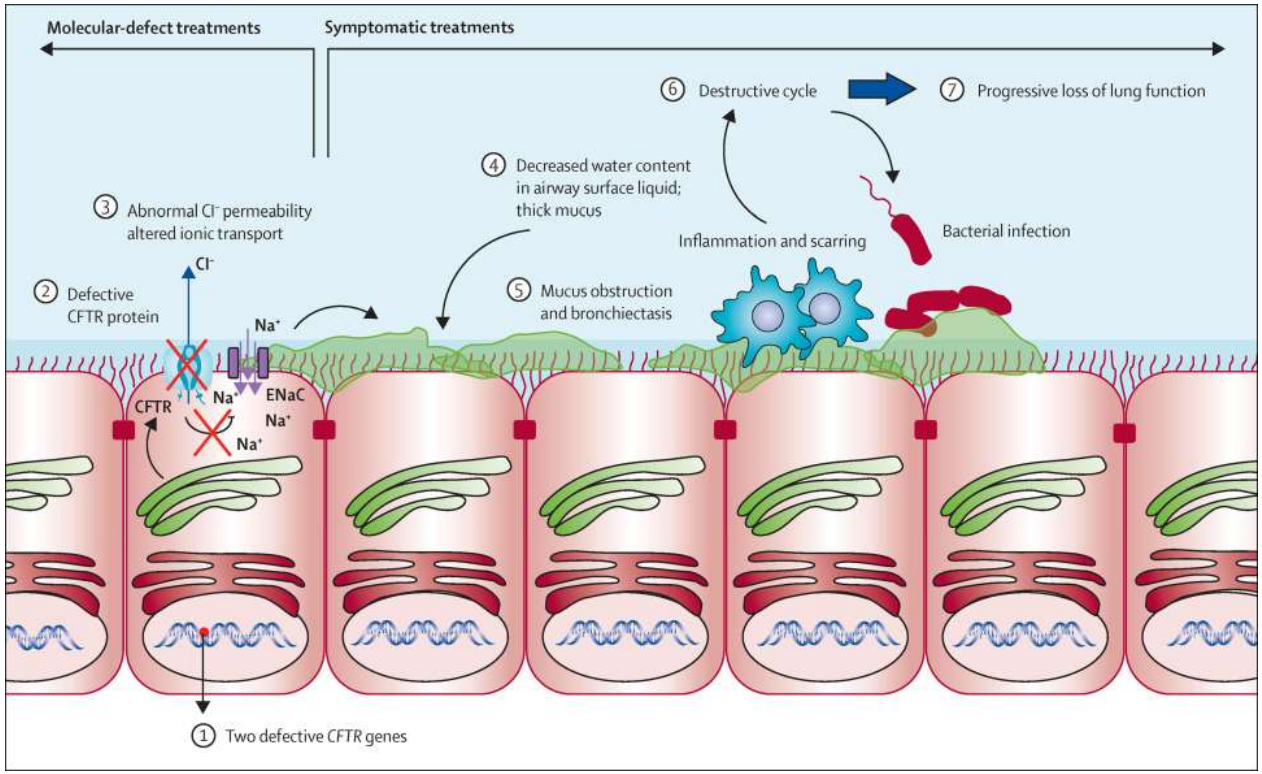

Figure 5. Pathogenic cascade of CF lung disease.

Mutations cause defective CFTR protein, resulting in reduced Cl^- secretion and an increase in Na^+ absorption. The impaired ion secretions lead to decreased water content in ASL, leading to thick mucus that the MCC cannot eliminate. Consequently, mucus obstruction occurs, allowing a destructive cycle of bacterial infection, inflammation, bronchiectasis, and tissue remodeling. This vicious cycle worsens lung function over time, resulting in progressive lung disease.

The figure was reprinted from "Progress in therapies for cystic fibrosis" by K. De Boeck and M.D. Amaral, *Lancet Respir Med*, (2016) [30].

DOI:10.14753/SE.2022.2632

1.2.2. Cystic fibrosis lung microbiome

Chronic airway infections are commonly polymicrobial. The most common bacteria found in the CF mucus are *Pseudomonas aeruginosa, Staphylococcus aureus, Haemophilus influenzae,* and *Burkholderia cepacia* [40, 41]. They are categorized as opportunistic pathogens that are highly harmful to immunocompromised and CF patients. In CF, chronic airway infections can occur at every stage of life. *S. aureus* and *H. influenzae* are commonly detected from the sputum in early ages. On the contrary, *P. aeruginosa* is often found later in the second or third decade of age [6, 41] (Figure 6).

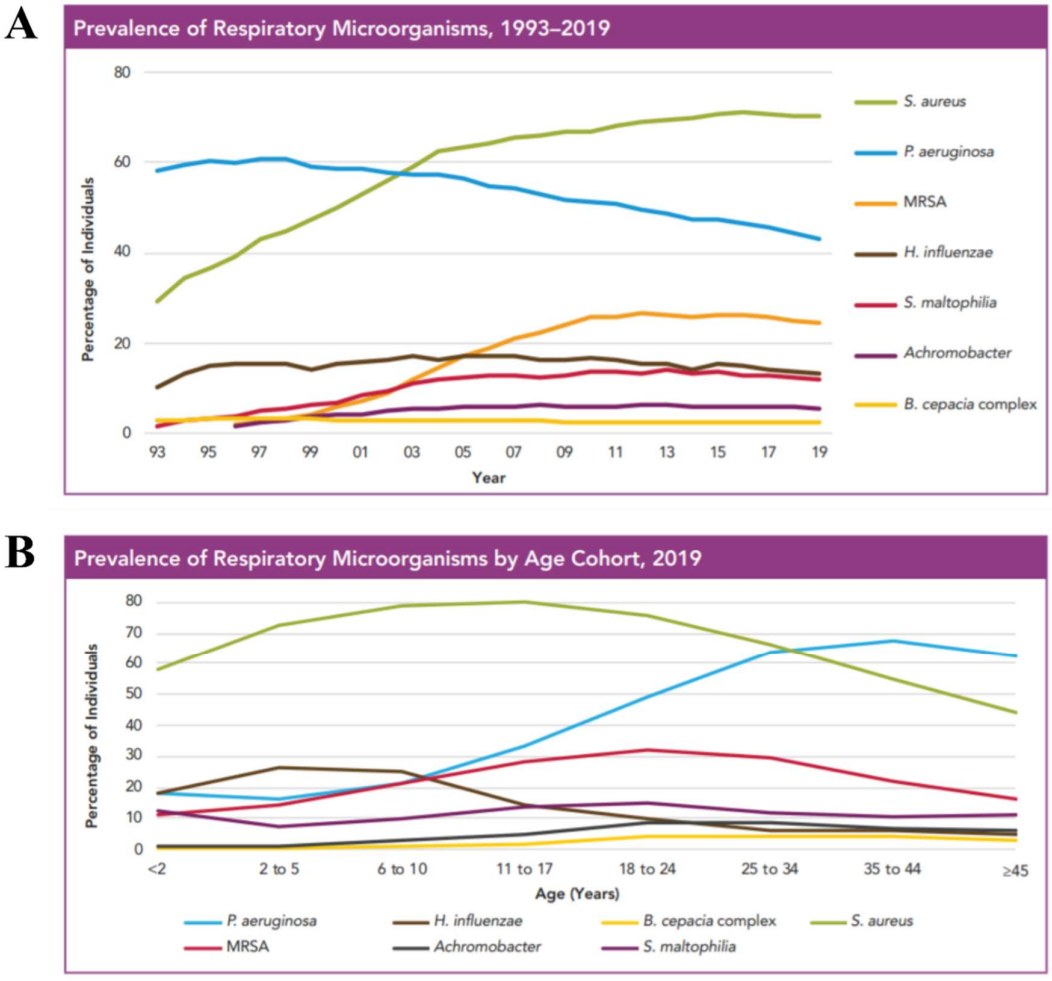

Figure 6. Prevalence of respiratory pathogens in patients with CF.

(A) Changing prevalence over time. **(B)** Prevalence by age. The figure was reproduced with permissions from Cystic Fibrosis Foundation Patient Registry: 2019 Annual Data Report, Bethesda, Maryland ©2020 Cystic Fibrosis Foundation [7].

It is still unclear how bacteria displace into the lower airways. Fothergill *et al.* suggest that the nasopharynx and upper airways are a silent reservoir of bacteria. Bacteria living in these areas can persistently adapt and migrate to the lower airways [42]. However, some studies suggest that aspiration could be the primary cause that leads pathogens from the nasopharynx to the lungs [43, 44].

Bacterial colonization in the lungs poses a significant threat for CF patients [45]. It is because CF bacteria can form biofilms, which persistently induce inflammation and worsen lung function. Bacterial biofilms are a mucoid surface-attaching lifeform of bacteria, consisting of communities of microorganisms in a self-produced polymeric matrix of variable composition, such as polysaccharides, proteins, lipids, and extracellular DNA. These materials provide structural stability, allowing bacteria to attach to the epithelial surfaces and mucin in the dehydrated mucus. Biofilms also provide bacteria protection from immune cells and antibiotics, making them resistant to host defense mechanisms. Aggressive antibiotic treatments are required to penetrate biofilm protection. However, this could also aggravate antibiotic resistance.

Notably, *P. aeruginosa* is well-known for its biofilm-production ability and is highly antibiotic-resistant due to its hypermutability [46]. Hypermutable bacteria usually produce different phenotype offspring that contain different genes. Some phenotypes are susceptible to antibiotics, but some are not. Thus, bacteria with the resistant phenotype may survive antibiotic exposure and subsequently dominate the communities. Moreover, horizontal gene transmission allows bacteria, even between different species, to share specific genetic information [47], especially resistance genes, making the whole biofilm community more resistant [48, 49].

In addition to bacteria, viruses and fungi are also microbiological agents that could be involved in developing lung diseases. Viral infection, for example, can trigger pulmonary exacerbations [33], whereas fungal infections by *Aspergillus fumigatus* and *Scedosporium apiospermium* are usually associated with allergic reactions (allergic bronchopulmonary aspergillosis) in CF [33, 50].

Microbial detection in the CF sputum is an excellent approach to identifying the bacterial species and determining the severity and management of the disease. Since *P.*

aeruginosa is highly mutable and capable of forming biofilms and associated with frequent hospitalizations and death [51], its detection is a truthful sign of the disease.

1.3. Role of bicarbonate in the airway surface physiology

Bicarbonate (HCO_3^-) is the second most abundant anion in the human body. The HCO_3^-/CO_2 buffering system is crucial in maintaining blood pH (pH~7.4), which is required for most cell functions. HCO_3^- is secreted in the duodenum to neutralize acidic chyme from the stomach in the digestive system. Alongside its buffering function, in the respiratory system, HCO_3^- is also considered as a CO_2 carrier, carrying a product of cellular respiration (CO_2) from cells to the lung tissues and releasing it during the gas exchange. Furthermore, HCO_3^- also plays a pivotal role in the airways regulating the airway surface epithelia and tertiary structure of the mucin molecules.

The airways are directly connected to the external environment and constantly exposed to microbes and foreign particles. Unlike the skin, the airway surface is lined with specialized ciliated epithelia covered with mucus keeping the surface clean. These pristine airways result from coordinating protective mechanisms, including the normal regulation of ASL, MCC, airway pH, mucus homeostasis, and lung immunity. All of these mechanisms seem to be linked to the proper secretion of HCO_3^- in the airways.

1.3.1. Airway surface liquid and mucociliary clearance

Airway surface liquid (ASL) is a thin layer of fluid, approximately 10 μm thick, covering the luminal side of the airway surface epithelia. It comprises two layers: (1) a periciliary liquid (PCL) layer, consisting of 96% water, 1% salts, 1% lipids, 1% proteins, and 1% mucus [52, 53], adjacent to the epithelium. This layer is impregnated with cilia from the epithelium. (2) a mucus layer (MCL) is a mucin-rich layer sitting atop of the PCL, exposed to the air in the lumen (Figure 7). The mucus layer consists of a heterogeneous mixture of macromolecules, including mucins, proteins, lipids, and cellular debris.

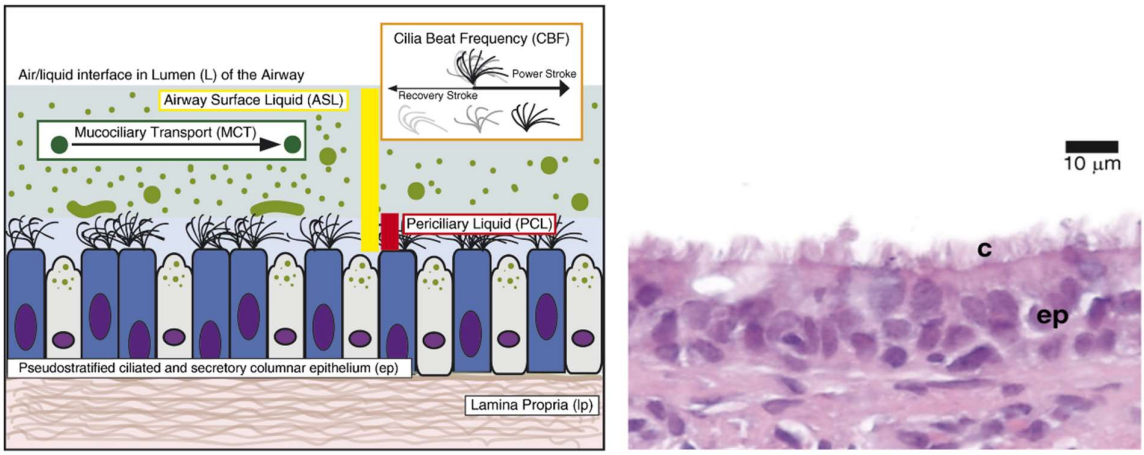

Figure 7. Airway surface liquid.

(left) Schematic illustration of airway epithelium structure and ASL. **(right)** hematoxylin and eosin histology of excised swine trachea. The figure was adapted with the permission of the American Thoracic Society. Copyright © 2021 American Thoracic Society. All rights reserved. Cite: Shei, R.J., Peabody, J.E., and Rowe, S.M. (2018). Functional Anatomic Imaging of the Airway Surface. *Ann Am Thorac Soc*. 15, S177-s183 [54].

MCL contains a large amount of gel-forming mucins, making it more viscous than the PCL. Since MCL sit on the top of the PCL, it can entrap inhaled microorganisms and particles. In contrast, PCL has less gel-forming mucins and is impregnated with cilia. Thus, PCL is more liquid and can be moved by the beating motion of cilia. This motion can upwardly sweep entrapped microorganisms and particles in the MCL to the upper airways to remove them from the lungs by the MCC [55, 56]. Moreover, membrane-bound mucins can be found in the PCL abundantly. These mucins tethered to epithelial cells' cilia and apical surface, forming a tight macromolecular mesh, preventing the penetration of inhaled particles and microbes in the airway epithelial cells [55].

In addition, ASL fulfills other vital functions in the airways (Table 1), such as humidification, buffering of the pH, lubrication, and it serves as a source of antimicrobial peptides. Therefore, maintenance of ASL homeostasis is critical and must be tightly regulated.

DOI:10.14753/SE.2022.2632

Table 1. Functions of respiratory tract fluid

Physical barrier to inhaled airborne organisms, particles, and other irritants, and aspirated foods and liquids
Entrapment of organisms, particles, and irritants
Formation of the vehicle on which irritants are transported by mucociliary action for clearance from the airways
Provision of a waterproof layer over the epithelium to limit desiccation
Humidification of inspired gas
pH buffering capacity
Lubrication
Insulation
Neutralization of toxic gases
Selective macromolecular sieve
Source of immunoglobulins and provision of extracellular surface for their activity
Source of antibacterial and other protective enzymes and provision of extracellular surface for their activity

This table was reprinted with permission from "Airway Surface Liquid: Concepts and Measurements," by John G. Widdicombe, in Rogers D.F., Lethem M.I. (eds) Airway Mucus: Basic Mechanisms and Clinical Perspectives. Respiratory Pharmacology and Pharmacotherapy. Birkhäuser, Basel. Copyright Springer Basel AG 1997 [57].

1.3.1.1. ASL composition and its regulation

In general, ASL consists of water, electrolytes, and macromolecules. Specifically, the PCL contains mostly water and salts, whereas macromolecules, such as proteins, glycoproteins, and cell debris, mainly accumulate in the MCL. The physiological regulation of these constituents results in healthy mucus that supports normal lung function.

1.3.1.1.1. Water and electrolytes

Numerous electrolytes, including H^+, Na^+, K^+, Cl^-, Ca^{2+}, PO_4^{3-} [57], and HCO_3^- [3], are detected in the ASL. These ions are maintained by various active and passive transport mechanisms, resulting in a certain level of inorganic strength. Studies suggest that the osmolality of ASL may be greater than that of body interstitial fluid, with values as high as 350 mOsmol/H_2O kg [58, 59]. This relatively high osmolality can pull water molecules into the epithelial cells and ASL via passive transport.

Water and electrolytes regulation occurs mainly in the PCL. It has been demonstrated that the thickness of PCL is accurately regulated. However, the total thickness of ASL (including the MCL) is varied among anatomical positions of the conduction airways, e.g., trachea, bronchi, and bronchioles [57, 60]. The optimal thickness of PCL is critical for the MCC efficacy, allowing cilia to reach the sheet of gel (MCL). On the contrary, it also keeps a distance between the cilia and gel, preventing the mucus gel from being pulled too tightly. Otherwise, the clearance might become ineffective.

Numerous ion and water channels are involved in transepithelial water and electrolyte transport in the lung. One of the most prominent transport proteins is the CFTR, which controls several transport mechanisms associated with electrolyte and fluid movement and pH regulation.

CFTR conducts both Cl^- and HCO_3^- according to their electrochemical gradient. Naturally, these anions have a relatively high hygroscopic property that can attract water molecules, resulting in water secretion to the airways. CFTR also inhibits ENaC activity, leading to decreased Na^+ reabsorption. Under physiologic conditions, Na^+ and Cl^- secretion is accompanied by fluid movement from the interstitial to the airways.

In addition to fluid movement, HCO_3^- secretion by CFTR also plays a significant role in regulating airway pH, which further influences mucus homeostasis, the property of antimicrobial peptides. This role will be extensively described in the airway pH regulation section.

1.3.1.1.2. Macromolecules

Mucin is the most abundant macromolecule in the ASL. In the normal airways, mucin serves as the chief substrate of mucus, covering and protecting the airway epithelia. Cell-surface or membrane-bound mucins (e.g., MUC1 and MUC4) are the mucins that tether to the surface of airway epithelial cells in the periciliary space to provide structural supports to cilia and the extracellular matrix [61] and form a physical barrier to protect the epithelium [62]. Gel-forming mucins (e.g., MUC5AC and MUC5B) are the mucins that form gelatinous substances, essential for protecting the epithelium and entrapping microorganisms and noxious substances and being a water reservoir for the PCL [60].

Gel-forming mucins are produced by goblet cells and submucosal glands of airway epithelia (Figure 8). They are naturally negatively charged. However, when packed and stored in the secretory granules (SGs), the negative charge is masked by protons and Ca^{2+}. Many studies suggest that HCO_3^- operates mucus secretion by chelating protons and Ca^{2+}. Once pH increases or Ca^{2+} is removed, the negative charges of mucin molecules repel each other, resulting in the expansion of mucin molecules (Figure 9) [63, 64].

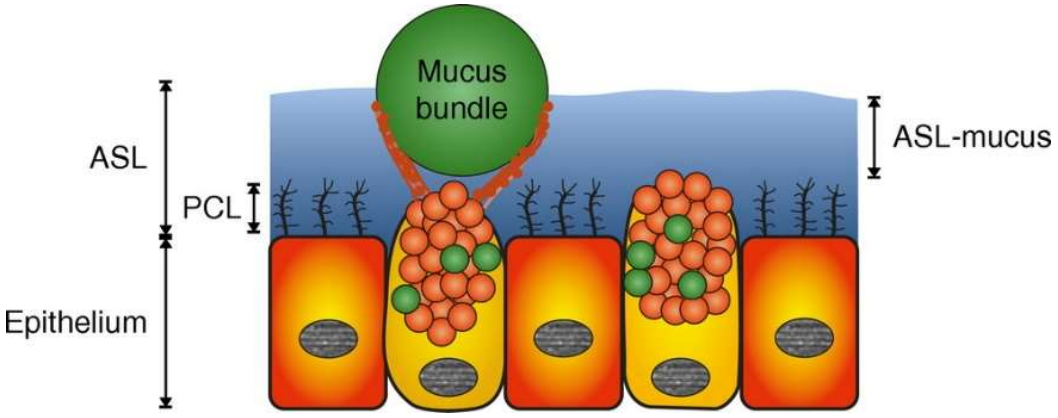

Figure 8. Schematic illustration of ciliated epithelium with goblet cells and ASL.
ASL consists of PCL and MCL (ASL-mucus). Goblet cells secrete MUC5AC (orange) and some MUC5B (green). The figure was adapted with the permission of the American Thoracic Society. Copyright © 2021 American Thoracic Society. All rights reserved. Cite: Ermund, A., Trillo-Muyo, S., and Hansson, G.C. (2018). Assembly, release, and transport of airway mucins in pigs and humans. *Ann Am Thorac Soc*. 15, S159-163. [64].

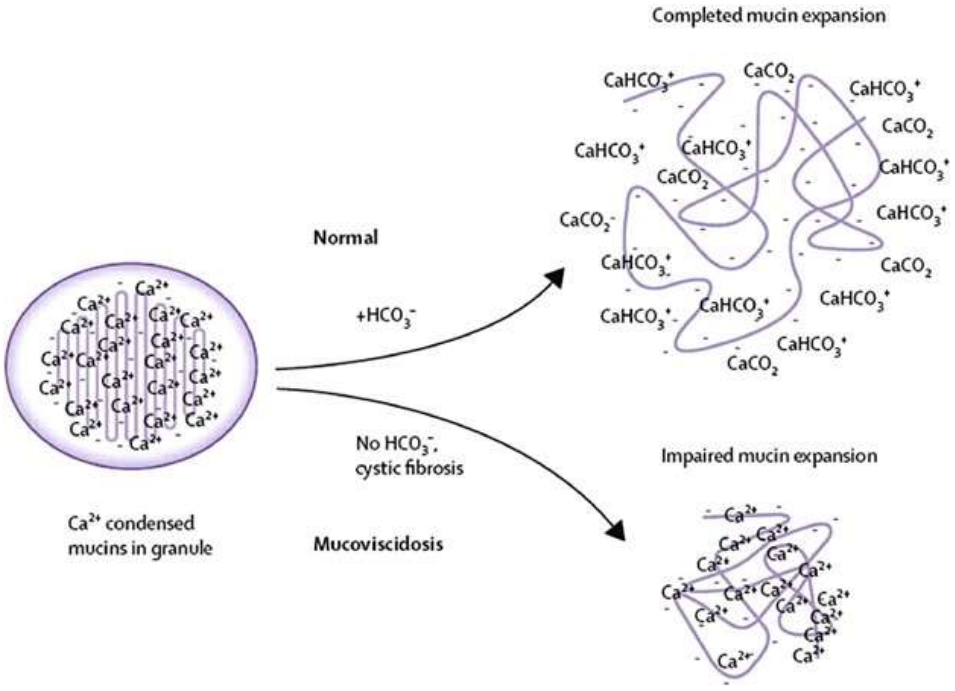

Figure 9. Schematic illustration of the mucin expansion by HCO_3^-.

Mucin granules masked by Ca^{2+} are chelated by HCO_3^- resulting in a completed mucin expansion, whereas in CF (mucoviscidosis), HCO_3^- secretion is limited, resulting in impaired mucin expansion. The figure was reprinted with permission from "Cystic fibrosis: impaired bicarbonate secretion and mucoviscidosis" by Quinton PM., *Lancet*, 2008. Copyright © 2008 Elsevier Limited [63].

Nonetheless, the SGs can also be regulated by extracellular ligands, such as inflammatory mediators, neurotransmitters, nucleotides, and nucleosides, all of which can be induced by either physiological or pathological mechanisms [61]. Therefore, irritants, changes in weather, seasonal allergies, or colds can induce mucus secretion in the upper airways [39].

Proteins such as albumin, lactoferrin, lysozyme, defensins, and immunoglobulins, as well as antimicrobial peptides, can be found in the ASL. They are primarily derived from plasma exudation or tissues, such as plasma cells and the airway epithelial cells.

The physiological regulation of these components results in healthy mucus production, which is simply cleared by the MCC. In pathological conditions, unusual materials linked to cellular damage and inflammation can be observed [57]. These materials include dead cells, fragments and debris, DNA, neutrophils, particles, and dead microbes. In fact, they are commonly found. However, their concentration is low. The accumulation of these materials due to infection or inflammation dramatically increases mucus viscosity, resulting in sticky mucus or sputum, which is hardly cleared by the MCC. Detection of these substances can be used as a biomarker for lung pathology.

1.3.2. Airway pH

ASL pH varies along the respiratory tracts. Studies suggest that in the lower airways, the ASL pH is approximately 7.0 ± 0.1 [62, 65, 66], and it becomes more acidic (5.6 – 6.7) in the upper airways. Tate *et al.* reported that the ASL pH of patients with stable CF was 5.88 and could lower to 5.32 during infective exacerbation [35]. However, the precise values of the airway pH are still debatable because the methods of pH measurement are diverse, and many factors can affect the results.

There are two main methods for measuring ASL pH. The optical methods use pH-dependent color changes of an organic dye (indicator) to measure the pH. On the other hand, the potentiometric methods use electrodes to measure the electrical voltage on the sample. Although the potentiometric methods seem to be more precise, many factors can interfere with the results. These include the immersion depth and placement of the electrodes, disturbance of epithelial layer, change in hygroscopicity, CO_2 concentration, temperature, and difference of cell type and experimental design [65].

ASL pH is buffered by a balance of acid-base reactions on the apical surface of the airway epithelia. The concentration of HCO_3^- and CO_2 are crucial that mainly determine the buffer capacity [67]. H_2CO_3 is the central intermediate species of the acid-base reaction (Figure 10). It is a weak acid generated by CO_2 and H_2O dissolution. However, this weak acid is unstable and constantly degraded to its deprotonated form, HCO_3^- and H^+, which can further react with hydroxide ion (OH^-), resulting in H_2O. These reactions occur dynamically and bi-directionally, creating a self-sustained HCO_3^-/H_2CO_3 buffering system that can tolerate minor pH interference.

DOI:10.14753/SE.2022.2632

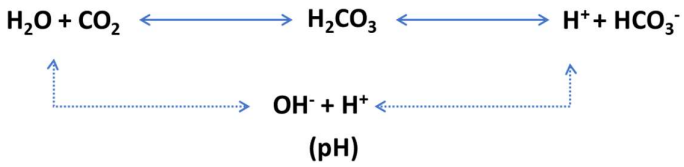

Figure 10. Bicarbonate/carbonic acid acid-base reaction.

The HCO_3^-/H_2CO_3 buffering system in the airway surfaces is maintained by tightly controlled HCO_3^- secretion. A recent theoretical model suggested that HCO_3^- secretion is regulated by CFTR, pendrin, and ANO1 and is aided by the coupling of Cl^- secretion (Figure 11) [65]. The primary source of HCO_3^- comes from the intracellular dissolution of CO_2 driven by the carbonic anhydrase enzyme (CA). Concurrently, H^+, the other product of CO_2 dissolution, is secreted by ATP-dependent active transporters onto the apical surface.

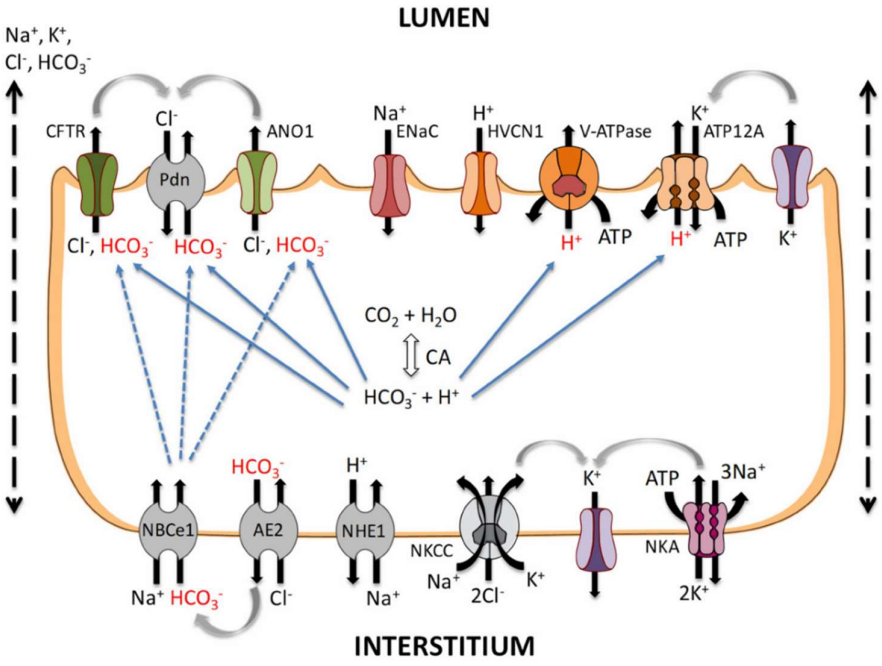

Figure 11. Distribution of the currently known transporters of airway epithelial cells.
HCO_3^- is secreted to the apical surface by CFTR, pendrin (Pdn), and ANO1, while H^+ is secreted by active transporters. Carbonic anhydrase (CA) activity is the primary source of HCO_3^- and H^+. Basolateral reabsorption and paracellular transport are also alternative sources of HCO_3^-. The figure was reprinted from "Airway Surface Liquid pH Regulation in Airway Epithelium Current Understandings and Gaps in Knowledge," by M. Zajac, *et al*., *Int J Mol Sci*, (2021)[65].

Additionally, HCO_3^- can be taken up by Na^+/HCO_3^- cotransporter (NBCe1) at the basolateral side of the epithelial cells. This transporter functions synergistically with Cl^-/HCO_3^- exchanger (AE2) to recycle HCO_3^-, which further enhances the driving force for apical HCO_3^- secretion. Paracellular HCO_3^- transport is also another pathway that helps to support apical HCO_3^- secretion when its concentration fluctuates. Moreover, other constituents, such as PO_4^{3-}, mucins, and some proteins also have a buffering property that can help to strengthen the buffering capacity in the ASL.

1.3.3. Innate airway immunity

Innate airway immunity involves several defense strategies that airway epithelial cells can use upon microbial challenges [68]. Recent studies suggest that HCO_3^- plays a vital role in these processes as well.

1.3.3.1. Protective mucus and the MCC

Airway epithelia are lined with ciliated cells. As previously described, these cells secrete membrane-bound mucins, which act as a physical barrier to the cells and physical support for cilia in the PCL of ASL. Gel-forming mucins secreted by globet cells and submucosal glands contribute to the airway mucus, entrap inhaled particles and microbes, and are further eliminated by the MCC [68].

HCO_3^- facilitates mucus homeostasis by triggering mucin expansion. It raises pH and chelates Ca^{2+}, which masks the SGs of mucins, resulting in a disperse of unfolding mucin molecules releasing to the mucus layer [63, 64]. Failure in HCO_3^- secretion has been shown to hamper mucus homeostasis in a piglet model [69]. Since HCO_3^- has a hygroscopic property that can raise the osmolality, HCO_3^- secretion also involves the fluid movement in the PCL, improving MCC.

1.3.3.2. Antimicrobial proteins

Antimicrobial proteins (AMPs) are abundantly detected in the ASL. They are secreted by airway epithelial cells and submucosal glands. The AMPs are effective against bacteria, viruses, and fungi that are entrapped in the mucus. AMPs are divided into two groups: small and large AMPs.

Small AMPs are short peptides with a positive charge. There are hundreds of them, but only two, defensins and cathelicidins, are found copiously in the ASL. These AMPs can induce microbial permeabilization [70] and have chemotactic activities that recruit the immune cells, such as mast cells, neutrophils, monocytes, macrophages, and T cells.

The other group of AMPs is large AMPs, which include lysozyme, lactoferrin, palate-lung-nasal-clone (PLUNC), and CCL20. Lysozyme was the first AMPs identified in ASL. It can induce the lysis of Gram-positive bacteria. Lactoferrin is known for its iron-sequestrating property, which reduces the concentration of free extracellular irons required for microbial metabolisms [71].

Normal AMP activities are linked to an optimal pH, which emphasis again the importance of HCO_3^- secretion in defense against the microbes. It has been reported that under acidic conditions, the bacterial killing capacity of AMPs is significantly decreased [36]. However, when ASL was supplemented with $NaHCO_3$, its bacterial killing capacity was restored [72]. These findings agree with data reporting that carbonate ions, including CO_3^{2-} and HCO_3^-, enhance AMPs activities [73].

1.3.3.3. Antimicrobial property of bicarbonate

Over the last decade, accumulated evidence has hinted that HCO_3^- has owned antimicrobial properties. It has been shown that natural mineral water that contains HCO_3^- can mitigate respiratory and skin infections [74]. In food and agricultural industries, HCO_3^- is used as an adjunctive microbial disinfectant and food preservative [75, 76]. In dentistry, HCO_3^- is added to dental care products, such as toothpaste and mouthwash, to reduce microbial accumulation and biofilm formation [77]. These findings have supported the antimicrobial property of HCO_3^-. However, it is still unclear whether this effect is due to its capacity to increase the pH or the anion *per se* has antimicrobial effects.

Furthermore, it is noteworthy that HCO_3^- concentration is precisely maintained in the human body. Therefore, the presumptive antimicrobial property could contribute to the general innate immunity of the human body.

DOI:10.14753/SE.2022.2632

1.4. Microbiological approaches in CF research

Chronic infections caused by opportunistic bacteria lead to pulmonary failure, the leading cause of death in CF. Therefore, researchers put significant effort into microbiology research to better understand the relationship between CFTR deficiency and bacterial colonization in the airways. Results of these investigations could contribute to the development of new therapeutic approaches in CF.

Culture-based methods are generally used to examine bacteria for diagnostic purposes or specific therapeutic agents or interventions. The culture-based methods are tied to microbiological media. Many microbiological media are nutrient-rich solutions that can favorably promote bacterial growth in a laboratory setting, yielding the best bacterial culture ready for investigations [78]. Most conventional microbiological media are non-selective. They are designed for universal use, and their composition is fixed so that most bacteria can grow in them.

However, when applying to CF microbiology, the reliability of using conventional microbiological media has been cast doubt since the composition of the CF lung secretion, in which CF bacteria colonize, is different from the traditional media. Accumulated data also support that CF bacteria behave distinctively in the lungs, suggesting the importance of the unique environment. These notions led to the development of alternative culture media that resemble the habitat in CF airways [79-82].

1.4.1. Artificial sputum medium

Artificial sputum medium (ASM) is a mucin-based medium resembling the CF airway environment. Its first record appeared in 1997 by Ghani and Soothil, as they intended to induce *P. aeruginosa* biofilm formation [79]. Since there has never been a consensus for the core recipe, various versions and modifications have been proposed. Sriramulu and colleagues pioneered the ASM study by investigating the effect of each ASM component and proposing the most comprehensive formula, containing mucins, free DNA, egg yolk emulsion, proteins, and electrolytes, as the main constituents [80]. Their finding later became the main guideline for creating ASM [83].

In the last decade, ASM has been applied in a broad range of studies. Accumulated evidence has proven its suitability in CF microbiology. CF pathogens grown in ASM tend to show their typical characteristics, including specific gene expression, microcolony (biofilm) formation, metabolite utilization, surface motility, evolutional diversity, and, most importantly, rigorous antibiotic-resistant ability, similar to those pathogens found in the CF lung [79, 80, 82, 84-90]. ASM has reduced the complexity of CF microbiology making it easily accessible in a laboratory setting.

1.4.2. Bacterial growth determination

In medical microbiology, observation of microbial growth is a common strategy to identify microbial infection or determine the efficiency of an intervention. Several methods are used for microbial growth determination.

1.4.2.1. Light-absorbing method

The simplest approach is the light-absorbing method. Bacteria grown in a solution are shed by the light of a specific wavelength generated by a spectrophotometer. A sensor on the other side detects the light that penetrates through the solution presenting as an optical density (OD) of the solution. The OD value varies depending on the turbidity of the solution that absorbs a certain amount of light. The more turbid, the higher value of OD, which directly links to the density or number of bacteria.

This method allows continuous monitoring of bacterial growth for days without interruption. However, it is noteworthy that bacterial culture is a mixture of live and dead cells and some other extracellular products that this method cannot distinguish. Therefore, the OD value may not represent the actual number of live bacteria. Moreover, the composition of the growth medium can also affect the OD value. For example, the medium's turbidity, color, or heterogenicity can increase the OD, which may mislead the results [86].

1.4.2.2. Viable cell count

The colony-forming unit (CFU) assay is the gold-standard method for viable bacterial cell count. Following treatment, the bacterial culture is diluted serially up to 10 - 12 sequential dilutions. Each bacterial solution is plated on an agar Petri dish and incubated overnight. The Petri dishes with countable colonies (approximately 25 to 250

colonies per Petri dish) are selected and counted for a total number of colonies. The number of colonies is calculated by multiplying with the dilution factor, giving the actual number of bacteria in the solution.

Since all bacteria in a colony originate from the same parental cell, they are considered an individual unit. Moreover, only intact bacteria can undergo cell division. Therefore, the number of bacteria/colonies obtained in this assay represents the number of living bacteria in the solution [91].

1.4.2.3. Flow cytometry

Flow cytometry is a technique that uses a laser beam shotting to the flow of cells or particles and detects the light scattering, revealing the cell's physical and chemical characteristics. With fluorescent labeling, this method enables cellular identification and detection of some specific material in the solution.

In microbiology, flow cytometry combined with nucleic acid double-staining (NADS) allows researchers to simultaneously distinguish and quantify living and dead cells [92, 93]. Bacterial cells are stained with a mixture of two different nucleic acid dyes; one is cell membrane-permeant, whereas the other cannot enter healthy cells. Cell-permeant dyes, such as Sybr Green and SYTO9, promptly penetrate the cell membranes and attach to the genetic materials. In contrast, cell-impermeant dyes, such as propidium iodide (PI), enter only cells with damaged membranes. Inside the cells, PI quenches Sybr Green or SYTO9 fluorescence.

This method is fast and provides reliable information about bacterial membrane integrity. However, it requires experienced technicians to monitor the measurement and analyze the data. Moreover, the quality of the results dramatically relies on the machine, analyzing software, and chemical reagents, which are costly. Biological factors, such as the cell membrane of the Gram-negative bacteria and bacterial growth stage, can also interfere with the results [94].

1.4.3. Biofilm formation quantification

The studies of biofilm formation have started in the 1980s when researchers found that most aquatic bacteria predominately attach to surfaces [95]. In medicine, biofilm

DOI:10.14753/SE.2022.2632

formation is usually associated with infections on the surface of medical implants or opportunistic infections in patients with immunocompromised immune or long-term hospitalization, as well as CF patients. Many methods have been developed to detect and quantify biofilm formation.

1.4.3.1. Biofilm crystal violet assay

Biofilm crystal violet assay is a simple, reliable, and quick method that allows *in vitro* quantification of bacterial biofilms. Bacteria are grown for at least 24 h allowing biofilm formation. The bacteria are subsequently removed, and the leftover attaches (biofilms) are stained with crystal violet (CV).

CV staining is nonspecific. It stains all biomass, both living and dead cells, as well as the matrix composed of extracellular polymeric substances [96]. Therefore, this method helps assess the overall biofilm response. However, it may not be appropriate to identify biofilms with living bacteria since it does not distinguish the living and dead cells.

DOI:10.14753/SE.2022.2632

2. Objectives

Although the antimicrobial property of HCO_3^- has been previously suggested, its direct effect on bacteria remains largely unknown. Thus, we have designed a series of experiments to investigate the antimicrobial effect of HCO_3^- *per se*. The experiments were performed both in conventional microbiological media and artificial sputum medium.

The main goals were:

1. To determine the most suitable preparation procedure and composition of ASM for these experiments.
2. To study the effects of HCO_3^- on the growth of *Staphylococcus aureus* and *Pseudomonas aeruginosa.*
3. To investigate the effects of HCO_3^- on biofilm formation of *Pseudomonas aeruginosa*.

DOI:10.14753/SE.2022.2632

3. Methods

3.1. Growth conditions for bacteria

3.1.1. Brain-heart infusion broth

Brain-heart infusion (BHI) medium (Mast Group Ltd., Merseyside, UK) (37 g/L) was prepared following the manufacturer's instructions. The pH was set to a pH of 7.4 with NaOH solution. The medium was subsequently aliquoted into four portions (Table 2 BHI). One portion was kept unchanged for the control sample. For the other three, either 100 mM NaCl or $NaHCO_3$ were added to make the designed conditions. All four media were autoclaved at 121°C for 30 min. $NaHCO_3$-containing BHI was always equilibrated with 5% or 20% CO_2 for at least 16 h at 37˚C before use.

3.1.2. Bouillon medium

Bouillon medium was prepared according to the following recipe: 0.3% meat extract, 0.2% yeast extract, 1% peptone, and 0.5% NaCl. The pH was adjusted to 7.5 with NaOH solution. The medium was divided into five portions (Table 2 Bouillon). One portion was kept unchanged for the control sample. Glucose (11 mM) [97] was added to the other four, then either 100 mM NaCl or $NaHCO_3$ were added to the medium according to the experimental design.

3.1.3. Artificial sputum medium

ASM used in our experiments was developed based on published literature (Table 3). ASM was prepared with four different conditions (Table 2 ASM_1). $NaHCO_3$-free ASM was used as control media, whereas $NaHCO_3$-containing ASM was assigned as the experimental media.

DOI:10.14753/SE.2022.2632

Table 2. Culture media and conditions

Media	Conditions	pH	NaCl (mM)	$NaHCO_3$ (mM)	Atmospheric conditions	Glucose	DNA	Test
BHI	(1) Control BHI	7.4	-	-	Ambient air	-	-	OD
	(2) 100 mM NaCl	7.4	100	-	Ambient air	-	-	
	(3) 100 mM $NaHCO_3$	8.5	-	100	5% CO_2	-	-	
	(4) 100 mM $NaHCO_3$	7.4	-	100	20% CO_2	-	-	
Bouillon	(1) Control bouillon	7.5	-	-	Ambient air	×	-	CVA
	(2) Glucose bouillon	7.5	-	-	Ambient air	✓	-	
	(3) 100 mM NaCl	7.5	100	-	Ambient air	✓	-	
	(4) 50 mM $NaHCO_3$	7.5	-	50	10% CO_2	✓	-	
	(5) 100 mM $NaHCO_3$	7.5	-	100	20% CO_2	✓	-	
ASM_1	(1) $NaHCO_3$-free	7.4	100	-	Ambient air	✓	✓	CFU & CVA
	(2) $NaHCO_3$-free	8.0	100	-	Ambient air	✓	✓	
	(3) 25 mM $NaHCO_3$	7.4	75	25	5% CO_2	✓	✓	
	(4) 100 mM $NaHCO_3$	8.0	-	100	5% CO_2	✓	✓	
ASM_2	(1) $NaHCO_3$-free	7.4	100	-	Ambient air	✓	×	FC
	(2) $NaHCO_3$-free	8.0	100	-	Ambient air	✓	×	
	(3) 25 mM $NaHCO_3$	7.4	75	25	5% CO_2	✓	×	
	(4) 100 mM $NaHCO_3$	8.0	-	100	5% CO_2	✓	×	

Ambient air = 0.04% CO_2

OD = optical density; CFU = colony-forming unit assay; CVA = crystal violet assay; FC = flow cytometry.

DOI:10.14753/SE.2022.2632

Table 3. Artificial sputum medium recipe developed from published literature.

Author	*Ghani & Soothill*	*Sriramulu et al.*	*Palmer et al.*	*Fung et al.*	*Kirchner et al.*	*Yeung et al.*	*Wright et al.*	*Behrends et al.*	*Quinn et al.*	*Comstock et al.*	*Davies et al.*	*Jaikumpun et al.*	Reference
Year	1997	2005	2007	2010	2012	2012	2013	2013	2015	2017	2017	**2020**	
mucin	0.5%	0.5%	-	1%	0.5%	1%	0.5%	0.5%	2%	2%	0.5%	**2%**	[88, 98]
DNA	4 g/L	4 g/L	-	1.4 g/L	4 g/L	1.4 g/L	4 g/L	4 g/L	1.4 g/L	1.4 g/L	4 g/L	**1.4 g/L**	[82, 85, 88, 98]
NaCl	90 mM Na^+ 30 mM K^+ 80 mM Cl^-	85 mM	50 mM	85 mM	85 mM	50 mM	85 mM	85 mM	85 mM	100 mM	85 mM	**100 mM**	[98]
KCl		30 mM	15 mM	30 mM	30 mM	15 mM	30 mM	30 mM	30 mM	30 mM	30 mM	**30 mM**	[83, 84, 88, 98]
Ferritin		-	-	-	-	-	-	-	3 µL/mL	3 µL/mL	-	**3 µL/mL**	[88, 98-101]
DTPA	5.9 mg/L	5.9 µg/mL	-	5.9 µg/mL	5.9 µg/mL	-	5.9 µg/mL	5.9 µg/mL	-	-	5.9 µg/mL	**-**	[88, 98]
Egg yolk	5 mL/L lecithin	5 µL/mL	-	5 µL/mL	5 µL/mL	-	5 µL/mL	5 µL/mL	0.01%	5 µL/mL	5 µL/mL	**5 µL/mL**	[83, 84, 98]
Essential amino acids		5 g/L	19 mM	5 g/L	2.5 g/L	1 g/L	2.5 g/L	5 g/L	7.225x	7.225x	2.5 g/L	**5 g/L**	[83]
Non-essential amino acids									14.45x	7.225x			
Glucose	-	-	3 mM	-	-	-	-	-	-	-	-	**11 mM**	[102]
Buffer	Tris	Tris	PO_4^{3-} & MOPS	Tris	Tris	PO_4^{3-}	Tris	Tris	PO_4^{3-}		Tris	**HEPES & $NaHCO_3$**	-
Other modifications		-	9.3 mM L-lactate, 2.3 mM NH_4Cl	10 mg/mL BSA	-	2 mM $MgSO_4$, 10 µM $FeSO_4$	-	-	-	Indicators	-	**$NaHCO_3$**	[102]
Sterilization	-	Autoclave	-	Antibiotics	Filtration	70°C 24h	Filtration	Filtration	Autoclave	Autoclave	Filtration	**Multiple techniques**	-

3.1.3.1. Preparation of ASM-ingredient stock solutions

A stock solution of each ingredient was prepared in advance in a large volume, then aliquoted into small portions, and stored in the refrigerator (4°C) (except for the DNA stock solution kept at -20°C). The concentration and sterilization technique of each ingredient stock solution are shown in Table 4.

Table 4. ASM components and their final concentration

Name	Stock Concentration	Final Concentration	Sterilization technique
Mucin from porcine stomach	5% (*w/v*)	2 % (*w/v*)	Autoclaving
DNA sodium salt from salmon testes	14 mg/mL	1.4 mg/mL	Dissolving in sterile deionized water
Casein hydrolysate	20 mg/mL	5 mg/mL	Filtration
Egg yolk emulsion	1x	0.005x	Instant sterile
Ferritin	1 mg/mL	0.003 mg/mL	Dissolving in sterile deionized water
NaCl*	2 M	100, 75 or 0 mM	Filtration
$NaHCO_3$*	1 M	0, 25 or 100 mM	Filtration
KCl	2 M	30 mM	Filtration
Glucose	2 M	11 mM	Filtration
HEPES acid	1 M	50 mM[#]	Filtration
HEPES sodium salt	1 M		Filtration

* Concentration of NaCl and $NaHCO_3$ are varied depending on the ASM conditions (Table 2).
[#] Appropriate volumes of HEPES acid and HEPES sodium salt are mixed to obtain the specific pH value (Table 5).

3.1.3.2. ASM preparation

3.1.3.2.1. $NaHCO_3$-free ASM (control ASM)

$NaHCO_3$-free ASM (pH 7.4 and 8.0) were prepared by mixing an appropriate volume of each ingredient-stock solution. The final concentration of each constituent is shown in Table 4. The pH of the $NaHCO_3$-free ASM was adjusted by adding HEPES acid and Na-HEPES stock solutions (Table 5). Sterile deionized water was added in the last step to bring up the final volume to 20 mL.

Table 5. buffering system and pH adjustment

pH	HEPES acid	HEPES sodium-salt	Total concentration
7.4	27 mM	23 mM	50 mM
8.0	12 mM	38 mM	50 mM

3.1.3.2.2. $NaHCO_3$-containing ASM

All ingredients, except NaCl, were mixed in the same method as the $NaHCO_3$-free ASM. To make 25 or 100 mM $NaHCO_3$ ASM, an appropriate volume of 1 M $NaHCO_3$ stock solution was added to the solution. Since the effect of ionic strength was concerned, we reduced NaCl concentration to 75 mM in the ASM containing 25 mM $NaHCO_3$ and to zero in the ASM containing 100 mM $NaHCO_3$ (Table 2 ASM_1) to maintain the osmolality (approximately 300 mOsm in total). Moreover, these $NaHCO_3$-containing ASM were incubated in 5% CO_2, according to Henderson–Hasselbalch equation, resulting in pH 7.4 and 8.0, respectively.

It is noteworthy that $NaHCO_3$ was naturally sensitive to heat and atmospheric conditions. Therefore, we prepared our ASM freshly, and $NaHCO_3$ was constantly added to ASM immediately before bacterial incubation.

For the flow cytometry experiment, DNA-free ASM was created because free DNA in ASM can interfere with the nucleic acid staining (Table 2 ASM_2). Thus, the DNA component was omitted and replaced by an equal volume of sterile deionized water.

DOI:10.14753/SE.2022.2632

3.2. Bacterial strains

Bacterial strains used in the experiments were *Staphylococcus aureus* (ATCC® 29213™) and *Pseudomonas aeruginosa* (ATCC® 27853™). The spectrophotometry and CFU were also carried out with two further isolates of the same species: *S. aureus* (SA-113) and *P. aeruginosa* (PA-17808). For the biofilm crystal violet assay, only *P. aeruginosa* clinical isolate (PA-17808) was tested because our pilot studies revealed that only this strain produced a detectable amount of biofilm. The list of all bacteria and the tests are shown in Table 6. The PA-17808 strain was obtained from the Central Bacteriological Diagnostic Laboratory of Semmelweis University, Budapest, while the SA-113 strain was originally isolated from an asymptomatic carrier by the workgroup of the Institute of Medical Microbiology, Semmelweis University, Budapest.

Table 6. List of Bacteria

Bacteria	Strains	Spectro-photometry	Colony-forming unit assay (CFU)	Flow cytometry	Biofilm crystal violet assay
S. aureus	ATCC® 29213™	✓	✓	✓	
S. aureus	SA-113	✓	✓		
P. aeruginosa	ATCC® 27853™	✓	✓	✓	
P. aeruginosa	PA-17808	✓	✓		✓

SA-113 and PA-17808 are clinical isolates

3.2.1.1. Preparation of bacterial suspensions

The pre-culture of each bacterium was prepared for each individual experiment from the same stock culture stored at -80˚C. Bacteria were plated onto simple agar plates and incubated overnight. Single colonies were then picked to inoculate into a 15-mL test tube containing 5 mL of Brain-Heart Infusion (BHI) broth (Mast Group Ltd., Merseyside, UK) and cultured overnight at 37˚C. The density of the cultures was adjusted to the desired value with a VITEK Densichek apparatus (Biomérieux, Marcy l' Étoile, France) directly before using them for the experiments.

3.3. Growth experiments

In this project, we used three different methods to determine bacterial growth under the presence and absence of $NaHCO_3$.

3.3.1. Light-absorbing method (Spectrophotometry)

3.3.1.1. Bacterial inoculation

Overnight culture of each bacterium was inoculated to each BHI condition to the density of 0.5 McFarland (approximately 1.0 x 10^8 cells/mL). The bacterial suspensions were mixed gently. 200 µL aliquots of each suspension were dispensed into 96-well plates in duplicate and incubated at 37˚C in ambient air (for $NaHCO_3$-free BHI), or in 5% or 20% CO_2 (for $NaHCO_3$-containing BHI) as designated.

3.3.1.2. Spectrophotometry measurement

The growth of bacteria was followed by measuring the optical density (OD) at 595 nm using a PR2100 microplate reader (Bio-Rad Laboratories, Hercules, Canada) 60 min after inoculating and subsequently every 15 min for 5.5 h. A negative control sample (without bacteria) was also prepared at the same time.

3.3.1.3. Data management

Values of OD from each condition were subtracted from the OD value of the negative control. The results of the parallel measurements of duplicate samples were averaged and normalized to the control media. Data in averaged OD values were plotted in a graph (OD vs. time). The growth rates were determined by calculating the area under the curve (AUC) [103] using Microsoft Excel, based on the summation of small trapezoids.

3.3.2. Colony-forming unit assay

3.3.2.1. Bacterial inoculation and cultures

Overnight cultures of each bacterium were adjusted to 3.0 McFarland (approximately 9.0 x 10^8 cells/mL) and inoculated at a 1:50 dilution into ASM and mixed gently. 200 µL aliquots of each suspension were dispensed into 96-well plates in triplicate and incubated at 37˚C in ambient air (ASM without $NaHCO_3$) or 5% CO_2 (ASM with $NaHCO_3$). After 6 or 17 hours of incubation, 30 µL of the bacterial culture was taken and serially diluted over a range of dilution factors from 10^{-1} to 10^{-9}. After that, 10 µL aliquots

of each dilution were plated onto simple agar plates. The plates were incubated at 37˚C overnight.

3.3.2.2. Bacterial enumeration

The colonies on each plate were counted by using ImageJ software (NIH, USA). Only plates that showed approximately 25 to 250 colonies were selected and subsequently calculated to CFU per milliliter (CFU/mL) with the following equation:

$$CFU/mL = \frac{(Number\ of\ counts\ on\ the\ plate)}{(0.01 \times Dilution\ factor)}$$

Results in CFU/mL were then converted to a logarithmic scale (log CFU/mL). In each condition, three independent experiments were carried out (n = 3). All data were pooled (totaling 9 replicates per treatment group, except for *S. aureus* ATCC at 6 h having only 3 replicates). The mean values of log CFU/mL in each condition were compared as designated.

3.3.3. Flow cytometry experiment

3.3.3.1. Bacterial cultures

Bacterial samples used in this experiment were prepared similar to the CFU assay. Briefly, overnight cultures were adjusted to 3.0 McFarland and subcultured at a 1:50 dilution into different DNA-free ASM conditions. 200 µL aliquots of each suspension were dispensed into sterile 1.5-mL tubes in triplicate and subsequently incubated for 17 h at 37˚C in ambient air or 5% CO_2.

3.3.3.2. Bacterial preparation and staining

After incubation, a 0.85% NaCl solution (1 mL) was added to each tube and centrifuged at 12,000 rpm for 2 min at room temperature (RT). The pellet was resuspended in 1 mL 0.85% NaCl solution and incubated for 10 min at RT. This step was repeated twice to remove excess ASM. Each bacterial suspension was then adjusted with 0.85% NaCl solution to 0.5 McFarland (approximately 1.5 x 10^8 cells/mL). In experiments with *P. aeruginosa*, EDTA (5 mM) was added to the saline solution to disrupt the bacteria's outer membrane and facilitate penetration of the dye [104].

Bacterial suspensions were stained with the LIVE/DEAD BacLight Bacteria Viability Kit (L7007, Invitrogen, Waltham, MA, USA). The BacLight consists of SYTO9, a membrane-permeant dye penetrating all cells, and PI, which is cell-impermeant and only enters damaged or dead cells. The staining reagent was prepared according to the manufacturer's instructions. Briefly, component A (1.67 mM SYTO9/1.67 mM PI) and component B (1.67 mM SYTO9/18.3 mM PI) were mixed 1:1 in a microtube. Five microliters of the mixture was added to 1 mL of each bacterial suspension (5 µL/mL final concentration). The suspensions were subsequently mixed thoroughly and incubated in the dark for 25 min before the measurement at RT. Microbeads (100 µL) (Invitrogen, USA) were added to the suspensions for cell quantification.

Samples containing ASM without bacteria were prepared and stained to determine background noise. The autofluorescence of the bacteria was assessed using unstained cells. The positive controls were generated by pre-treating the cells with propanol (70% (*v/v*)) to cause membrane damage and maximize PI penetration. Therefore, the membrane-damaged or dead cells were simply detected with the high intensity of PI.

3.3.3.3. Flow cytometric measurement

Flow cytometry was carried out using BD FACSCalibur system (Becton Dickinson, San Jose, CA, USA) equipped with a 635-nm Red diode laser and a 15-mW 488-nm air-cooled argon solid-state laser. Forward (FSC) and side scatter (SSC) were collected from 488 nm excitation. SSC was set as a discriminator to reduce electronic background noise during the analysis.

The instrument settings were defined by the Megamix-Plus SSC beads (Biocytex, Marseille, France) and optimized with 1 µm Silica Beads Fluo-Green Green (Kisker Biotech GmbH & Co., Steinfurt, Germany). Stained bacteria were excited by the 488-nm laser, and the fluorescence was collected through a 530/30-nm bandpass filter (SYTO9) and a 670-nm long-pass filter (PI).

All signals were amplified logarithmically (four decades). The sampling rate was adjusted to less than 1,000 particles/s. Each measurement lasted 1 minute. Sterile PBS was applied as a sheath fluid. Data were acquired with BD CellQuest Pro software

(Becton Dickinson, San Jose, CA, USA). Stained cell suspensions were analyzed immediately after dye incubation.

3.3.3.4. Flow cytometry data analysis

Data gating and analysis were performed using Flowing software version 2.5.1 (Turku Centre for Biotechnology, Turku, Finland, released 4.11.2013). Dot plots of detected signals from each sample were analyzed based on the FSC, SSC, green (FL1), and red (FL3) fluorescence intensities (Figure 12).

A standardized bacterial gate (R-0) was set on the FSC-SSC dot plot, based on the Megamix-SSC boundary, to select the bacterial population (Figure 12 A, purple). This bacterial R-0 gate was then saved and applied to other samples. Next, the unstained, propanol-treated, and untreated ($NaHCO_3$-free) samples were analyzed to determine the regions of autofluorescence, dead, and living cells, respectively (Figure 12 B-D). Briefly, signals detected from the unstained sample were identified first and attributed to autofluorescence and background noise. They were subsequently gated in R-1 (Figure 12 B, grey signals) to discriminate them from bacterial signals. Next, the positive control and untreated samples were analyzed. Signals with high intensities in FL1 and FL3 (SYTO9- and PI-positive signals, respectively) were selected and attributed to bacterial cells (Figure 12 C&D).

DOI:10.14753/SE.2022.2632

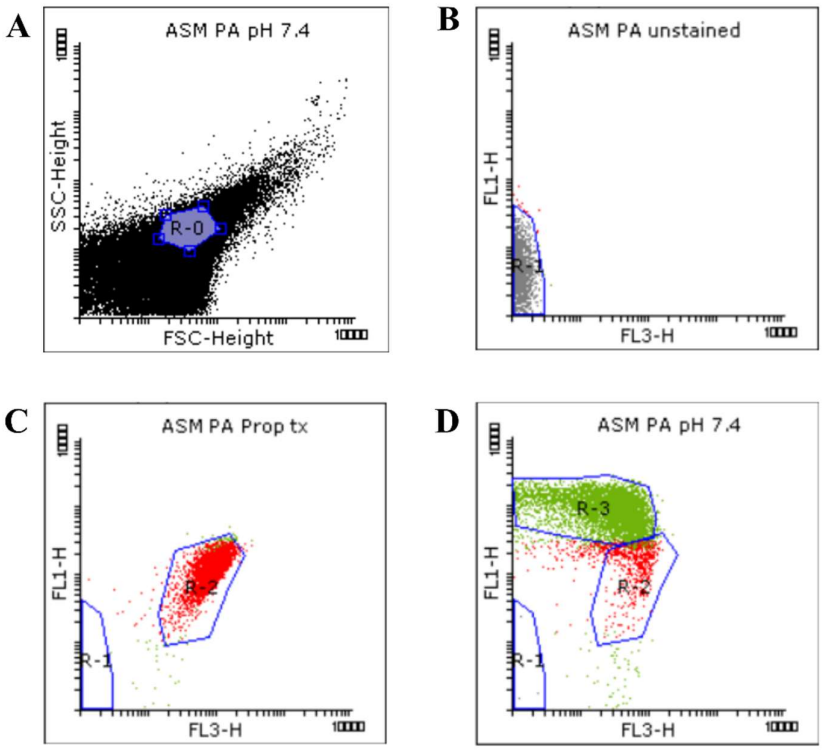

Figure 12. Gating strategy for the flow cytometric measurement.

Viability was determined by membrane integrity analysis using the LIVE/DEAD BacLight Bacteria Viability Kit. We defined a standardized bacterial gate (R-0) **(A)** on the FSC-SSC dot plot on the basis of the Megamix-SSC boundary. The bacterial signals inside the R-0 gate of the unstained **(B)**, propanol-treated **(C)**, and untreated (NaHCO3-free) samples **(D)** were analyzed based on the FL1 vs. FL3 fluorescence. Autofluorescence signals were gated in R-1. Signals with high FL3 intensity were gated in R-2. Signals with high FL1 intensity were gated in R-3.

To determine bacterial viability, manually set gates were applied based on the positive control and untreated samples. Since the positive control samples were treated 70% propanol to kill the bacteria, the signals detected from this sample, exhibiting a high intensity in FL3, were attributed to membrane-damaged or dead cells and gated in the R-2 region (Figure 12 C, red signals). This R-2 gate was next applied to the untreated samples, where signals outside the R-2 gate, which exhibited a high intensity in FL1, were gated in the R-3 region (Figure 12 D, green signals) and attributed to membrane-intact or healthy cells. The presets of these R-regions were saved as a template and then applied to the other samples using the automated folder runner function to obtain the data from each sample.

Frequencies of the signals inside the R-2 and R-3 gates from each condition were quantified using the statistic function of the software and presented as percentages of the total population in R-0. Three (*P. aeruginosa*) and four (*S. aureus*) independent experiments were performed. All data were pooled (totaling 9–12 replicates per treatment group). Means of the percentages of SYTO9- and PI-positive signals and the ratio of SYTO9- to PI-positive signals were compared in ASM with and without $NaHCO_3$.

3.4. Biofilm experiments

3.4.1. Crystal violet assays

Bacterial suspensions of *P. aeruginosa* (PA-17808) were prepared with the same methods as the other measurements. For the experiments with conventional culture media (bouillon), 100 µL aliquots of each suspension were dispensed into 96-well plates in eight-duplicate and incubated at 37˚C in ambient air ($NaHCO_3$-free condition), or in 5% or 20% CO_2 ($NaHCO_3$-containing condition) for 48 h.

For the ASM, 200 µL aliquots of each suspension were dispensed into 96-well plates in five parallel. Bacteria were incubated in ambient air (ASM without $NaHCO_3$) or 5% CO_2 (ASM with either 25 or 100 mM $NaHCO_3$) for 48 h at 37 °C.

3.4.1.1. Crystal violet staining and data collection

After incubation, unattached bacteria were removed by rigorous washing with 200 µL of 1× PBS three times. Bacteria attached to the wells were air-dried and stained with 125 µL crystal violet solution (0.1%) for 10 min. Excess crystal violet was removed by rinsing the plates several times in tap water. The plates were then air-dried. Crystal violet stain was solubilized in 30% acetic acid (200 µL/well) for 10 min. From each well, 125 µL of this solution was taken and transferred to a new flat-bottom 96-well plate.

Optical density (OD) was measured at 595 nm in a PR2100 microplate reader. The average OD from the control wells without bacteria was subtracted from the ODs measured in wells with bacteria. Three independent experiments were performed. All data were pooled. Means of OD in each condition were compared in the media with and without $NaHCO_3$ as designated.

3.5. Statistical analysis

Data from the experiments performed in the conventional media (BHI and bouillon) were analyzed using Statistica for Windows 7.0 (Statsoft). Data presented are means ± SD. The values were compared using ANOVA followed by an LSD *post hoc* comparison test. Changes were considered statistically significant at $p < 0.05$.

For the ASM, the statistical analysis was performed on the pooled data of each experimental group, except for *S. aureus* ATCC 29213 CFU assay at 6 h, by using GraphPad Prism version 8.0.0 (GraphPad Software, Inc., San Diego, CA, USA). Pooled data were normally distributed (Shapiro–Wilk test) and presented as means ± SD. The means were compared using one-way ANOVA, followed by Tukey's post-hoc multiple comparison test. The un-pooled data were analyzed by using Kruskal–Wallis test, followed by Dunn's post-hoc multiple comparison test. Changes were considered statistically significant if $p < 0.05$.

DOI:10.14753/SE.2022.2632

4. Results

4.1. Effects of bicarbonate on the growth of bacteria prevalent in CF

4.1.1. Bicarbonate inhibits the growth of *S. aureus* and *P. aeruginosa* in BHI

The growth rate of both *S. aureus* and *P. aeruginosa* was significantly reduced in BHI broth supplemented with 100 mM $NaHCO_3$ equilibrated with 20% CO_2 (pH 7.4) compared to $NaHCO_3$-free BHI at the same pH value (Figure 13).

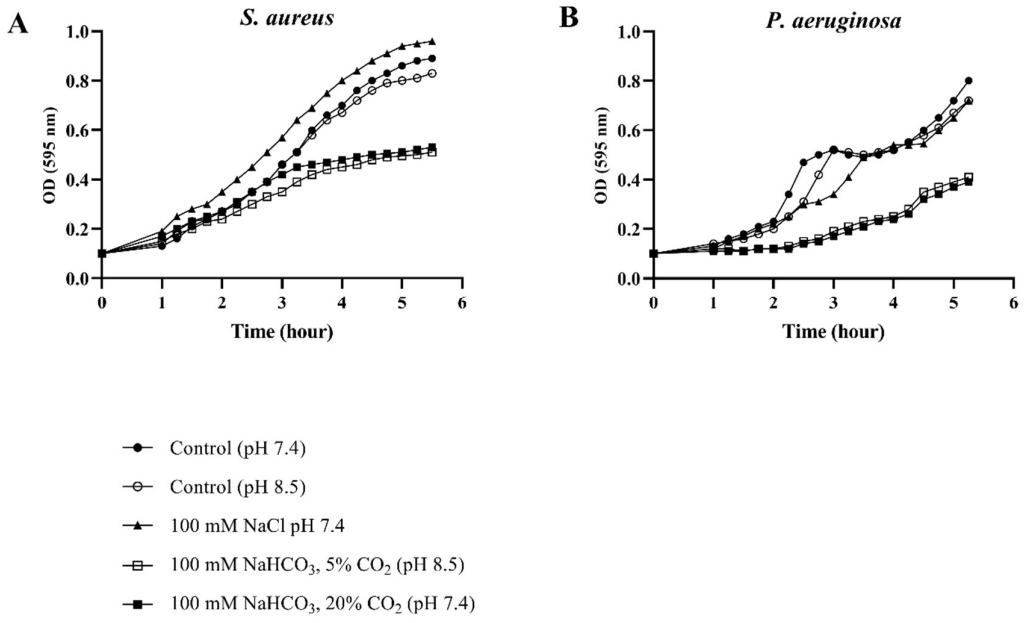

Figure 13. Bacterial growth rate in BHI medium with different conditions.
Growth of *S. aureus* **(A)** and *P. aeruginosa* **(B)** in BHI medium supplemented with $NaHCO_3$ compared to control conditions measured by the spectrophotometry technique. Each curve shows the average of two parallel experiments. Standard Deviations were generally less than 1% of the mean and are not shown.

Since the supplementation of 100 mM $NaHCO_3$ increased ionic strength, which may contribute to the growth reduction, we used BHI supplemented with 100 mM NaCl (pH 7.4) as control and incubated the bacteria for 6 h. Interestingly, the growth rate of both species was not affected in the NaCl-containing BHI, suggesting that the inhibitory effect of $NaHCO_3$ was not due to increased osmolality or ionic strength (Figure 13, black triangle).

However, the growth inhibition was also observed in the alkaline BHI (pH 8.5) supplemented with 100 mM $NaHCO_3$ equilibrated with 5% CO_2, prompting the query if the alkalinity of $NaHCO_3$ could affect the bacterial growth. Therefore, $NaHCO_3$-free BHI (pH 8.5) was also tested. We found that the growth capacity was not affected in $NaHCO_3$-free BHI (pH 8.5) (Figure 13, white dot *vs.* white square). Additionally, the inhibitory effect in $NaHCO_3$-containing BHI (pH 8.5) was similar to that observed in $NaHCO_3$-containing BHI pH 7.4 (Figure 13, black & white squares), indicating that the inhibitory effect was not due to alkaline pH.

The area under the curve (AUC) was calculated to compare the growth rates of bacteria in each condition quantitatively. For both species, the $NaHCO_3$-enriched medium resulted in approximately 25 to 50% AUC reduction compared to the medium without $NaHCO_3$ (Table 7).

Table 7. Calculated AUC values based on growth curves in Figure 13.

Bacterium	BHI (pH 7.4)	BHI (pH 8.5)	100 mM NaCl (pH 7.4)	100 mM $NaHCO_3$ (pH 7.4)	100 mM $NaHCO_3$ (pH 8.5)
S. aureus	2.48	2.41	2.93	1.92	1.76
P. aeruginosa	2.05	1.92	1.82	1.01	1.06

4.1.2. Bicarbonate decreases the CFU of *S. aureus* and *P. aeruginosa* in ASM

Artificial sputum medium mimics the CF airway environment. Thus, we investigated the growth of both *S. aureus* and *P. aeruginosa* in ASM. Our data show that the viable cell counts for both bacteria were significantly reduced in the ASM containing 100 mM $NaHCO_3$ (pH 8.0) compared to $NaHCO_3$-free ASM (pH 8.0) following 6 h incubation (Figure 14 A-D). In ASM supplemented with 25 mM $NaHCO_3$ (pH 7.4), only *P. aeruginosa* ATCC 27853 cell counts were significantly reduced (Figure 14 C).

DOI:10.14753/SE.2022.2632

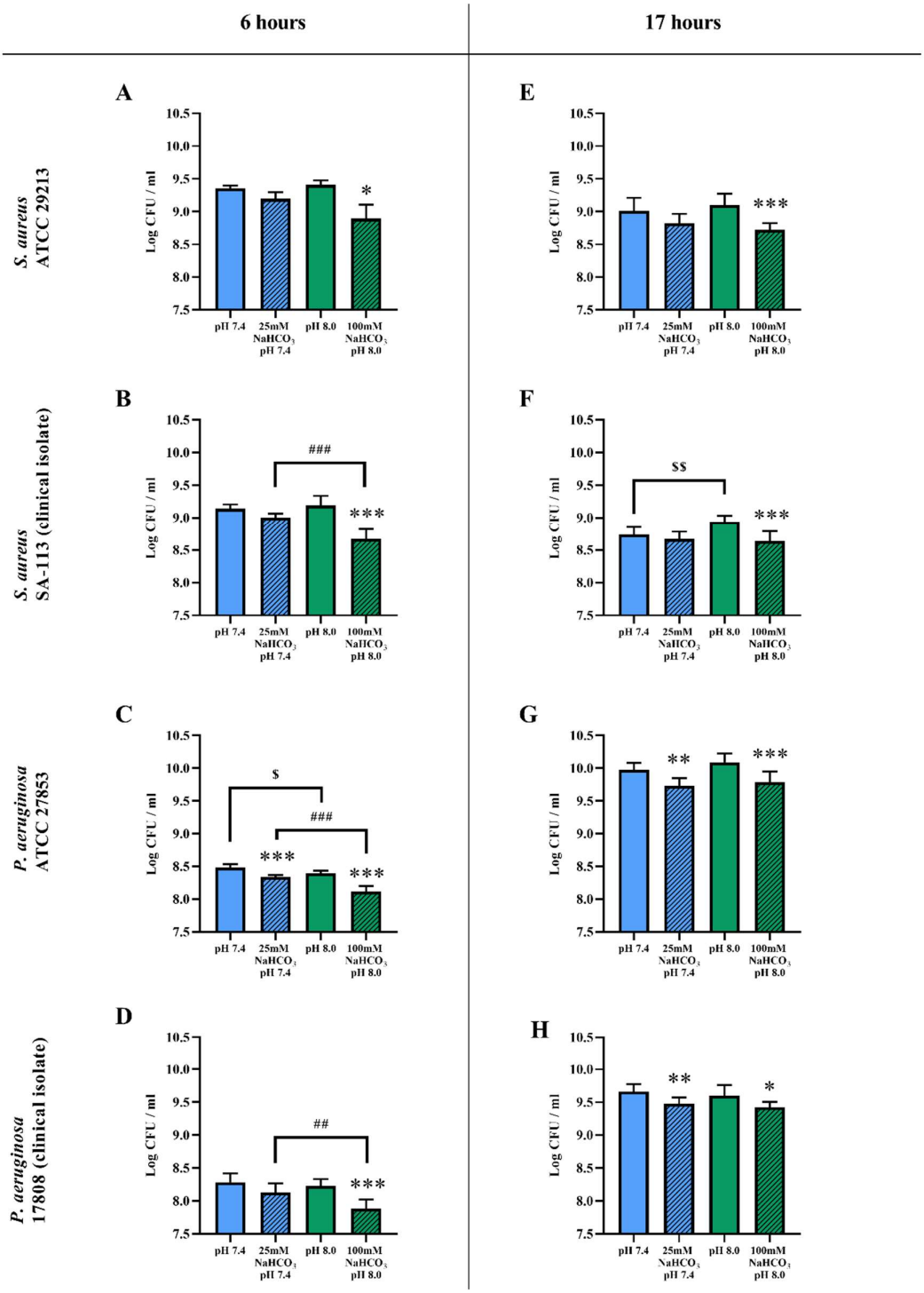

Figure 14. CFU assay of cystic fibrosis bacteria.

S. aureus ATCC 29213 (**A&E**), *S. aureus* SA-113 (**B&F**), *P. aeruginosa* ATCC 27853 (**C&G**), and *P. aeruginosa* PA-17808 (**D&H**) grown in different ASM conditions for 6 (**A-D**) and 17 h

(**E-H**) in ambient air or 5% CO_2. Values are presented as means of log CFU/ml ± SD. The experiment was repeated three times. All data were pooled, totaling 9 replicates per treatment group, except for *S. aureus* ATCC at 6 h having only 3 replicates (**A**). Statistical analysis: one-way ANOVA followed by Tukey's post-hoc multiple comparison test (**B-H**) or Kruskal-Wallis test followed by Dunn's post-hoc multiple comparison test (**A**). * = $p < 0.05$, ** = $p < 0.01$, *** = $p < 0.001$ when comparing ASM with and without $NaHCO_3$ at the same pH (**same-colored columns**); ## = $p < 0.01$, ### = $p < 0.001$ when comparing the two $NaHCO_3$ concentrations (25 vs. 100 mM) (**shaded columns**); $ = $p < 0.05$, $$ = $p < 0.01$ when comparing $NaHCO_3$-free ASM at pH 7.4 and 8.0 (**clear columns**).

After a 17 h incubation, similar inhibitory effects of $NaHCO_3$ were observed (Figure 14 E-H). The viable cell counts for both *S. aureus* and *P. aeruginosa* were significantly decreased in the ASM containing 100 mM $NaHCO_3$ (pH 8.0). However, in ASM containing 25 mM $NaHCO_3$ (pH 7.4), only viable cell counts for *P. aeruginosa* (both the ATCC strain and the clinical isolate) were significantly reduced (Figure 14 G&H).

Comparing the two $NaHCO_3$-containing ASM (25 *vs.* 100 mM $NaHCO_3$), the viable cell count reduction caused by 100 mM $NaHCO_3$ was significantly greater than that caused by 25 mM $NaHCO_3$ at 6 h incubation (with the single exception of the *S. aureus* ATCC strain). These results suggest a concentration-dependent inhibitory effect of HCO_3^- on bacterial growth (Figure 14 B-D). However, after the more prolonged incubation (17 h), no significant difference between the inhibitory effects of 25 and 100 mM $NaHCO_3$ was detected in either species (Figure 14 E-H).

Next, we asked whether the differences in pH of the $NaHCO_3$-containing media could influence the inhibitory effects of sodium bicarbonate. Therefore, we compared the bacterial counts in $NaHCO_3$-free ASM (pH 7.4 vs. pH 8.0). In the absence of $NaHCO_3$, the more alkaline (pH 8.0) medium did not decrease the *S. aureus* cell counts compared to the pH 7.4 (Figure 14 A,B,E). Interestingly, the counts were actually increased at pH 8.0 in the *S. aureus* clinical isolate following the 17 h incubation (Figure 14 F). On the other hand, the more alkaline pH slightly reduced the *P. aeruginosa* ATCC cell count after the 6 h incubation (Figure 14 C), but there was no significant difference following 17 h incubation (Figure 14 G). For *P. aeruginosa* clinical isolate, there was no significant

difference in the viable cell counts between $NaHCO_3$-free ASM pH 7.4 and 8.0, regardless of incubation time (Figure 14 D&H).

Taken together, our CFU data suggest that $NaHCO_3$ has a concentration-dependent inhibitory effect on bacterial growth, which is not due to changes in external pH.

4.1.3. Bicarbonate decreases the number of viable cells and increases membrane-damaged cells detected by the flow cytometry

We used the flow cytometry and LIVE/DEAD BacLight Bacteria Viability Kit to assess the effect of $NaHCO_3$ on the membrane integrity of the *S. aureus* and *P. aeruginosa* ATCC strains grown in different ASM conditions. BacLight is a combination of two nucleic acid stains (SYTO9 and Propidium iodide (PI)). These two dyes enter bacterial cells differently depending on the integrity of the cell membranes. SYTO9 can penetrate the intact cell membrane emitting green fluorescence (530 nm). In contrast, PI can only enter cells with damaged membranes. Once PI enters the cells, it quenches the SYTO9 fluorescence resulting in strong red fluorescence (670 nm). Therefore, cells with high intensity of green fluorescence (SYTO9) are considered healthy or viable, while red fluorescence indicates damaged or dead cells.

4.1.3.1. Flow cytometric dot plot

As a positive control, we used propanol to treat the bacteria. Indeed, when bacteria were treated with propanol (70% (v/v)), the strong red signal was detected (R-2) while the green signal (R-3) was absent (Figure 15 A&F), indicating that membrane damage leads to an increase in PI and decrease of SYTO9 signals.

Importantly, $NaHCO_3$ induced significant changes in density and shape of the clusters of SYTO9 and PI-positive cells (Figure 15 BC, DE, GH, IJ). Both 25 and 100 mM $NaHCO_3$ increased the intensity of the PI signals and decreased the intensity of the SYTO9 signals, which indicates that $NaHCO_3$ increased the bacterial membrane permeability.

DOI:10.14753/SE.2022.2632

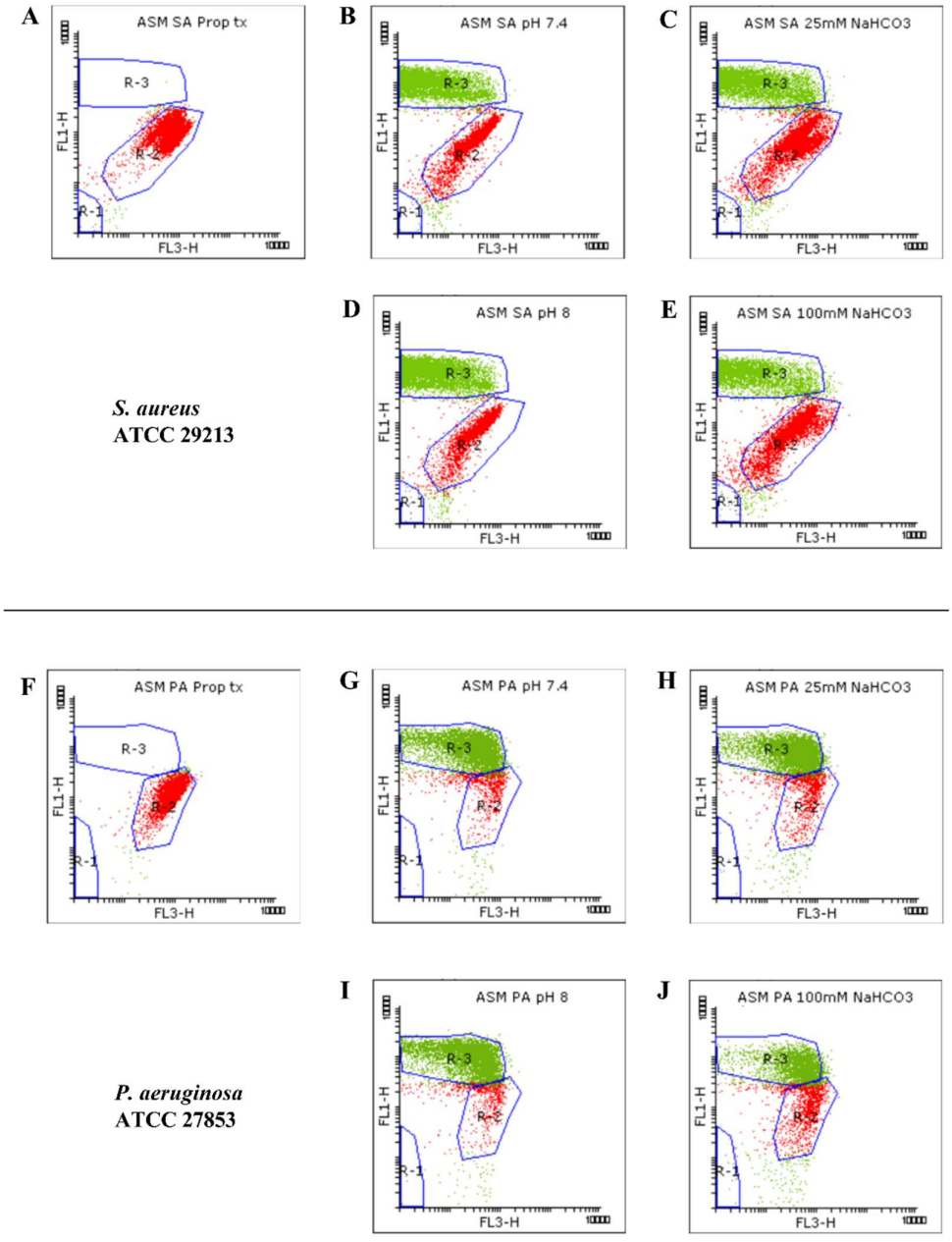

Figure 15. Flow cytometric dot plot of viability staining.

S. aureus (SA) and *P. aeruginosa* (PA) were cultured in ASM and treated with 70% propanol for membrane permeabilization (**A&F**), in $NaHCO_3$-free ASM (pH 7.4) (**B&G**), in ASM containing 25 mM $NaHCO_3$ (pH 7.4) (**C&H**), in $NaHCO_3$-free ASM (pH 8.0) (**D&I**), and in ASM containing 100 mM $NaHCO_3$ (pH 8.0) (**E&J**). Bacterial signals from each condition are plotted as dot plots (FL1 vs. FL3). SYTO9-positive (green), PI-positive (red), and autofluorescence signals were gated in R-3, R-2, and R-1, respectively.

4.1.3.2. Quantification of SYTO9 and PI-positive cells

Next, we quantified the SYTO9 and PI-positive cells and calculated the percentage of each cluster relative to the whole population. The percentage of SYTO9 and PI-positive cells in ASM with and without $NaHCO_3$ were compared at different pH values (Figure 16).

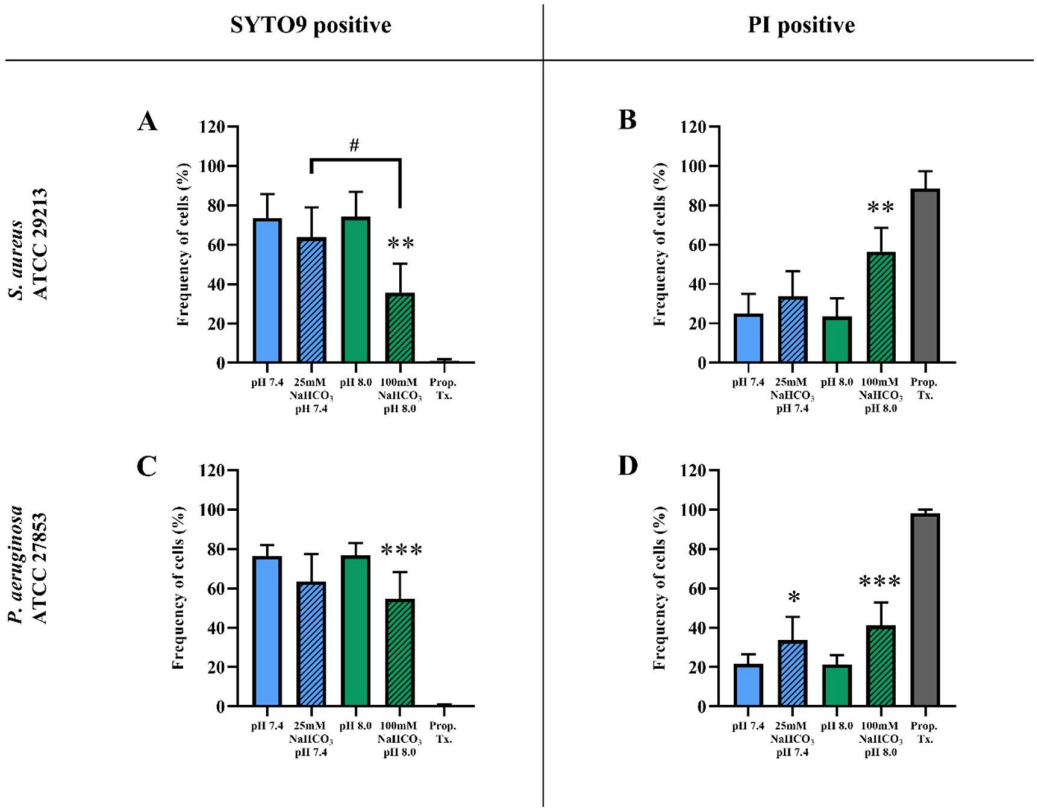

Figure 16. Percentage of SYTO9- and PI-positive signals.

Values are calculated from SYTO9- and PI-positive clusters of *S. aureus* ATCC 29213 (**A&B**) and *P. aeruginosa* ATCC 27853 (**C&D**) grown in different ASM after 17 h of incubation, and presented as a mean percentage ± SD. The experiment was repeated three (*P. aeruginosa*) or four times (*S. aureus*), totaling 9 - 12 replicates per treatment group). Statistical analysis: one-way ANOVA followed by Tukey's post-hoc multiple comparison test. ** = $p < 0.01$, *** = $p < 0.001$ when comparing ASM with and without $NaHCO_3$ at the same pH (**same-colored columns**); # = $p < 0.05$ when comparing the two $NaHCO_3$ concentrations (25 vs. 100 mM) (**shaded columns**).

We found a significant reduction in the percentage of SYTO9-positive cells for both *S. aureus* and *P. aeruginosa* in the ASM containing 100 mM $NaHCO_3$ (pH 8.0)

when compared to $NaHCO_3$-free ASM at the same pH (pH 8.0) (Figure 16 A&C). In contrast, the percentage of PI-positive cells was significantly increased in the ASM containing 100 mM $NaHCO_3$ for both species as well, when compared to $NaHCO_3$-free ASM at the same pH (pH 8.0) (Figure 16 B&D). Interestingly, in *P. aeruginosa*, a significant increase in the percentage of PI-positive cells in ASM containing 25 mM $NaHCO_3$ (pH 7.4) was also detected when compared to $NaHCO_3$-free ASM at the same pH (pH 7.4) (Figure 16 D).

In addition, we observed a concentration-dependent decrease in the percentage of SYTO9 positive *S. aureus* cells when compared the effects of 25 mM $NaHCO_3$ (pH 7.4) and 100 mM $NaHCO_3$ (pH 8.0) (Figure 16 A). In fact, this concentration-dependent pattern could be detected for the percentage of SYTO9 positive *P. aeruginosa* cells and the percentage of PI-positive of both bacteria species. However, differences did not reach the level of statistical significance. Furthermore, the ratios of SYTO9 to PI-positive cells of both bacteria species remain unchanged in $NaHCO_3$-free ASM regardless of pH (pH 7.4 vs. 8.0) (Figure 17). These results suggest that the effects of $NaHCO_3$ were not due to the alkalinization of the medium.

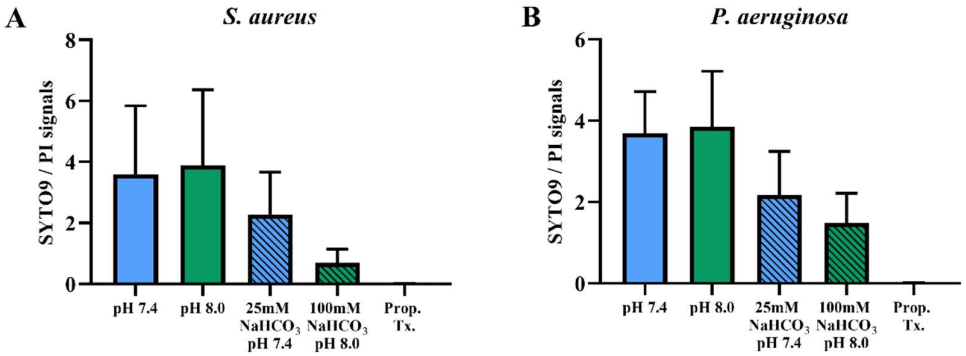

Figure 17. Ratios of SYTO9- to PI-positive signals.

S. aureus ATCC 29213 (n = 4) (**A**) and *P. aeruginosa* ATCC 27853 (n = 3) (**B**) in different ASM media. Values are presented as means ± SD.

DOI:10.14753/SE.2022.2632

4.2. Effects of bicarbonate on *P. aeruginosa* biofilm formation

4.2.1. Bicarbonate inhibits biofilm formation in conventional medium

Robust biofilm formation was observed in the $NaHCO_3$-free bouillon following 48 h of incubation, whereas biofilm formation was almost completely inhibited in bouillon containing either 50 or 100 mM $NaHCO_3$ (Figure 18). Moreover, to investigate whether the increase in osmolality could inhibit biofilm formation, we tested the effects of 100 mM NaCl (pH 7.5). Surprisingly, the NaCl-containing medium drastically increased biofilm formation compared to that observed in $NaHCO_3$-containing bouillon media, suggesting that the inhibition of biofilm formation was due to the effect of HCO_3^- *per se*.

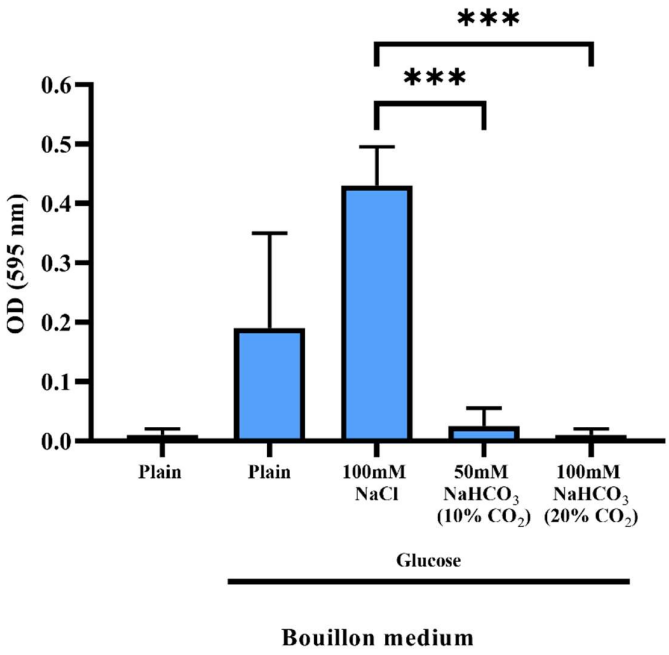

Figure 18. Biofilm formation capacity of *P. aeruginosa* in glucose-containing bouillon in the presence of NaCl or two different concentrations of $NaHCO_3$.

Please note that, in the absence of glucose, no biofilm formation was observed. *** $p < 0.001$.

DOI:10.14753/SE.2022.2632

4.2.2. Bicarbonate inhibits biofilm formation in ASM

We observed that $NaHCO_3$ inhibited *P. aeruginosa* biofilm formation in ASM. We detected a massive *P. aeruginous* biofilm formation in $NaHCO_3$-free ASM following 48 h incubation. In contrast, biofilm formation was significantly inhibited in NaHCO3-containing ASM (both 25 and 100 mM) (Figure 19). Interestingly, the alkaline $NaHCO_3$-free ASM (pH 8.0) increased biofilm formation (Figure 19 B, clear columns). This evidence reinforces the assumption that the high pH does not inhibit biofilm formation.

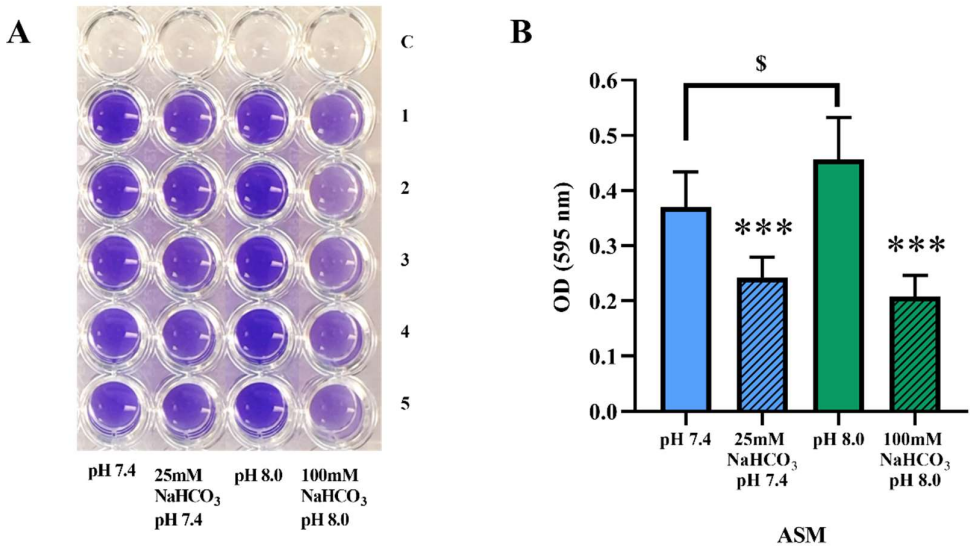

Figure 19. Biofilm formation capacity of *P. aeruginosa* grown in different ASM.
(A) crystal violet staining after *48* h of incubation. **(B)** statistical analysis of biofilm formation. Values are presented as means of optical density (OD) ± SD. The experiment was repeated three times (n = *3*, *15* replicates per treatment group). Statistical analysis: one-way ANOVA followed by Tukey's post-hoc multiple comparison test. *** = $p < 0.001$ when comparing ASM with and without $NaHCO_3$ at the same pH (same-colored columns); $ = $p < 0.05$ when comparing the $NaHCO_3$-free ASM at pH *7.4* and *8.0* (clear columns).

DOI:10.14753/SE.2022.2632

5. Discussion

In these studies, we investigated the effects of HCO_3^- on the growth and biofilm formation of prevalent CF bacteria both in conventional microbiological and artificial sputum medium. We found that HCO_3^- inhibits the growth of *S. aureus* and *P. aeruginosa* in both media. Furthermore, HCO_3^- reduces *P. aeruginosa* biofilm formation. Our results suggest that these antimicrobial effects are independent of pH changes and could be due to bacterial membrane damage caused by HCO_3^- *per se*.

5.1. Antimicrobial property of bicarbonate

CFTR dysfunction leads to impaired HCO_3^- transport which compromises lung functions [36]. HCO_3^- plays a pivotal role in regulating the volume and composition of the airway surface liquid [63, 64, 105]. In addition, the antimicrobial properties of HCO_3^- have been discussed for several decades [74-77]. However, it is still unclear whether these antimicrobial effects of HCO_3^- are due to alterations in pH or ionic strength.

We first tested the effects of HCO_3^- on prevalent CF bacteria (*S. aureus* and *P. aeruginosa*) in different BHI media (Figure 13). The results showed that 100 mM HCO_3^- significantly reduced the growth rates of both *S. aureus* and *P. aeruginosa*. This confirmed the antimicrobial effects of HCO_3^-. In addition, the antimicrobial effects seem to be independent of pH and osmolality because the growth rates were not affected in BHI controls (with an equal amount of NaCl supplementation at the same pH).

Defective HCO_3^- secretion in the CF lungs contributes to the production of pathological mucus (sputum) [63], which is ideal for bacterial colonization [37, 40]. It has been demonstrated that CF mucus can induce the expression of the genes associated with biofilm formation, which is very different from those found in the traditional media [80]. Therefore, we used a special medium (ASM) mimicking the composition of CF sputum [79, 80]. Previous data showed that ASM is suitable for CF microbiological studies [79, 80, 82, 84-90]. However, none of the existing ASM recipes included HCO_3^- in the composition. Therefore, in order for us to observe the effects of HCO_3^-, we had to modify the ASM composition explicitly for our experiment slightly.

The preparation of ASM containing $NaHCO_3$ is very challenging. HCO_3^- is naturally unstable and possesses a proton buffering capability, which can strongly alkalinize pH. On the other hand, changes in pH and/or atmospheric CO_2 concentration can also dissipate HCO_3^- content. In fact, HCO_3^-, pH, and CO_2 levels are interconnected, forming a chemically inseparable triad relationship, in which one of the parameters cannot be modified without changing the other two. Thus, reliable control of these parameters becomes a classic obstacle for researchers dealing with HCO_3^- [106]. Besides, it is noteworthy that HCO_3^- can be easily destroyed by other chemicals during the preparation or pH adjustment. In addition, at low CO_2 levels, HCO_3^- can sharply increase the pH to a deadly range for the cells.

We solved this problem by applying three different strategies. First, we worked at 5% CO_2 regardless of HCO_3^- concentrations of the ASM. According to the Henderson-Hasselbalch equation, using 25 or 100 mM HCO_3^- at 5% CO_2 results in a pH of ~7.4 or ~8.0, respectively. Second, to strengthen the HCO_3^-/CO_2 buffer system, we added HEPES buffer for an additional buffering system in $NaHCO_3$-containing ASM. We also used HEPES buffer for the control media (HCO_3^--free ASM pH 7.4 or 8.0). Third, to avoid HCO_3^- degeneration, all ASM were always freshly prepared, and HCO_3^- was added into the ASM immediately before bacterial inoculation. Using these approaches, we could have four different and comparable ASM conditions (Table 2 ASM). Therefore, we investigated the effects of HCO_3^- on CF bacteria under conditions more resembling the CF airway environment.

We first assessed the bacterial growth in ASM by using spectrophotometry, similar to our prior experiments with the BHI medium. However, the first attempt was not successful because ASM was naturally turbid. In addition, ASM contained a high amount of macromolecules, such as mucins and DNA, which tend to precipitate over time. Since the spectrophotometer estimates the number of bacteria by detecting the light intensity at a given wavelength, turbidity of the ASM and precipitation significantly interfered and misled the results [86]. Therefore, we used the colony-forming unit (CFU) assay and flow cytometry to investigate the bacterial growth in ASM. The results obtained by these two different methods were similar, confirming our previous observations in the BHI medium using spectrophotometry.

The viable cell count assay is the gold-standard method to quantify the number of bacteria. We used this approach by incubating the bacteria in ASM with and without HCO_3^- for 6 and 17 h. Our results show that 100 mM HCO_3^- significantly decreased the viable cell counts of *S. aureus* and *P. aeruginosa* in ASM in both 6 and 17 h (Figure 14), indicating that the bacterial growth in the exponential and stationary phases was inhibited. These findings confirmed our previous results suggesting the antibacterial property of HCO_3^-. Notably, similar observations have also been reported in food sciences. The growth rate of food-contaminating bacteria, such as *E. coli*, *L. plantarum*, and *S. aureus*, as well as *P. aeruginosa*, can be significantly reduced by 120 mM $NaHCO_3$. This effect is even more pronounced on yeasts [76]. Another study suggests that $NaHCO_3$ can exert antimicrobial effects when its concentration reaches or exceeds 25 mM [107].

Moreover, we investigated the effects of HCO_3^- at two different concentrations (25 mM and 100 mM). As expected, the higher concentration of HCO_3^- exerted a more potent effect (Figure 14 B-D). However, these dose-dependent inhibitory effects seem to be present only during the exponential growth phase. After 17 h incubation, both concentrations were equally effective (figure 14 E-H). The explanation of these phenomena is unclear. We hypothesize that this may be due to the natural features of HCO_3^-. First, HCO_3^- is bacteriostatic, and extended incubation time with spectrophotometry revealed that bacterial growth fully recovered after 24 h [102]. Second, as mentioned earlier, HCO_3^- is also unstable by nature. Environmental factors, such as changes in pH (H^+ concentration) or CO_2, can change its concentration. Third, all variables and parameters, including HCO_3^-, were only set initially, then we let the experiments run with no interruption. Therefore, taken together, prolonged incubation could result in a significant loss of HCO_3^-, which allows an increase in the bacterial growth rate.

However, these scenarios are entirely different from the normal airways, where the physiological concentration of HCO_3^- is steadily maintained. Although the estimated physiological concentration is relatively low (10 - 20 mM) [62], persistent HCO_3^- secretion in the normal airways could sustain this concentration, resulting in ever available antimicrobial effects against microbial challenges in the lungs.

In parallel with the CFU assay, a more advanced technique, the flow cytometry combined with nucleic acid double-staining (NADS), was used to assess bacterial viability [92, 93]. In ASM containing 100 mM $NaHCO_3$, the percentage of damaged cells (PI-positive) increased, while the intact cells (SYTO9-positive) decreased for both *S. aureus* and *P. aeruginosa* (Figure 16). These findings are in agreement with data obtained in CFU assay and spectrophotometry, supporting the antimicrobial effects of HCO_3^-. However, initial experiments with *P. aeruginosa* (a Gram-negative bacterium) were unsuccessful. We observed that SYTO9 was unable to penetrate through the membrane of *P. aeruginosa*. This phenomenon has been previously reported by other studies suggesting that the outer membrane of Gram-negative bacteria constitutes a barrier preventing SYTO9 permeation [94, 104, 108]. Nevertheless, this problem can be solved by an appropriate dose of UVA light, glutaraldehyde, or EDTA [104, 109]. We used 5 mM EDTA to facilitate the SYTO9 entry to *P. aeruginosa* cells.

Data obtained by flow cytometry uncovered a possible mechanism of action of HCO_3^-. Our results showed that HCO_3^- could alter the percentage of PI- and SYTO9-positive cells, suggesting that HCO_3^- may cause bacterial membrane damage. A recent study suggests that HCO_3^- may dissipate the proton gradient on the bacterial membrane, resulting in membrane instability, reducing viability [106]. Another explanation is that HCO_3^- may chelate divalent cations (e.g., Ca^{2+} and Mg^{2+}), necessary for bacterial membrane stability [110, 111].

As mentioned previously, EDTA enhanced SYTO9 penetration into *P. aeruginosa*. Some studies suggest that EDTA could have antimicrobial effects [112-114]. Thus, we speculate that these effects also result from the chelation of cations [115].

5.2. Biofilm-suppressing effects of bicarbonate

In the CF airways, where HCO_3^- secretion is impaired, pathogenic bacteria tend to form biofilms representing a significant threat for CF patients. We first investigated the effects of HCO_3^- on *P. aeruginosa* biofilm formation in Bouillon (conventional) medium supplemented with 2% glucose. We found that 100 mM HCO_3^- inhibited the biofilm formation while equimolar NaCl (100 mM) had no effect (figure 18). Our findings are in line with data published by Gawende and colleagues reporting that *P. aeruginosa*

biofilms were suppressed by $NaHCO_3$ combined with sodium metaperiodate and sodium dodecyl sulfate [116]. Pratten and colleagues also reported that $NaHCO_3$ could disrupt oral biofilm *in vitro* [117].

Since the composition of the medium could influence bacterial behavior and biofilm formation capacity [79, 80], we repeated these experiments in ASM. ASM containing 25 and 100 mM $NaHCO_3$ significantly inhibited *P. aeruginosa* biofilm formation (figure 19). These results strengthen the clinical relevance of our previous observations, indicating that HCO_3^- suppresses bacterial conversion to biofilm lifestyle.

Interestingly, a significant increase in *P. aeruginosa* biofilm formation was detected in alkaline $NaHCO_3$-free ASM (pH 8.0). This finding agrees with the other studies demonstrating increased biofilm formation in alkaline pH [118, 119]. Nevertheless, considering that alkaline pH significantly stimulates biofilm formation, we speculate that HCO_3^- suppresses biofilm production independent of its alkalinizing effects on pH.

5.3. Bicarbonate as a therapeutic agent

Since CF is a genetic disease, it is understandable that most attention and resources have been devoted to developing CFTR protein correctors and modulators. Nowadays, numerous CFTR modulators exist. However, they can be used only for certain CFTR defects (Figure 4). For example, ivacaftor is developed for class III mutations.

Although the overall outcomes of protein-modulator/corrector treatments are promising [120], the disease progression cannot be stopped. Pulmonary exacerbations and other complications can still occur [16, 30]. Pulmonary exacerbation and other complications still remain at nearly the same rate as they have historically [7]. Moreover, all CFTR defects are still not covered since more than 2,000 mutations exist, and several more are still unidentified. Therefore, conventional symptomatic therapies are still required.

For CF lung disease, the symptomatic therapies are based on three key aspects; restoration of ASL and MCC, reduction of lung inflammation, and efficient control of chronic lung infections [30]. Thus, several drugs explicitly targeting different symptoms have been introduced to improve CF treatments. For example, Dornase alfa, a DNAse

mucolytic agent, is used to increase mucociliary clearance. Non-steroid anti-inflammatory drugs (NSAIDs) are used to mitigate inflammation. Antibiotics, indeed, are prescribed for both prevention and alleviating bacterial infection. Therefore, CF patients have to take a combination of drugs for their entire life. This is a considerable burden, and possibly other complications can develop, such as antibiotic resistance [121].

Inhalation of $NaHCO_3$ containing aerosols has caught attention since recent evidence has revealed the link between HCO_3^- deficiency and CF lung disease's pathogenesis. Restoration of HCO_3^- levels in CF airways may be a pivotal factor to improve CF morbidity and mortality. Many *in vitro* and *in vivo* studies support this idea. It has been shown that HCO_3^- can increase airway pH [122], improve airway viscosity and MCC [69, 105, 123, 124], and restore airway bacterial killing capacity [72]. Our data demonstrate concentration-dependent antimicrobial effects of HCO_3^- inhibiting bacterial growth and biofilm formation.

Moreover, a recent clinical study evaluating the safety, tolerability, and effects of inhaled aerosolized $NaHCO_3$ solution (4.2% and 8.4%, which is equivalent to 50 and 100 mM) in CF volunteers suggests that both HCO_3^- concentrations are safe, significantly increase airway pH, and can reduce the sputum viscosity [125]. An *in vitro* study conducted by our team also supports that 100 mM $NaHCO_3$ was well-tolerated by both wild-type (WT-CFTR CFBE) and CF bronchial epithelial (ΔF508-CFTR CFBE) cells (Figure 20) [126].

DOI:10.14753/SE.2022.2632

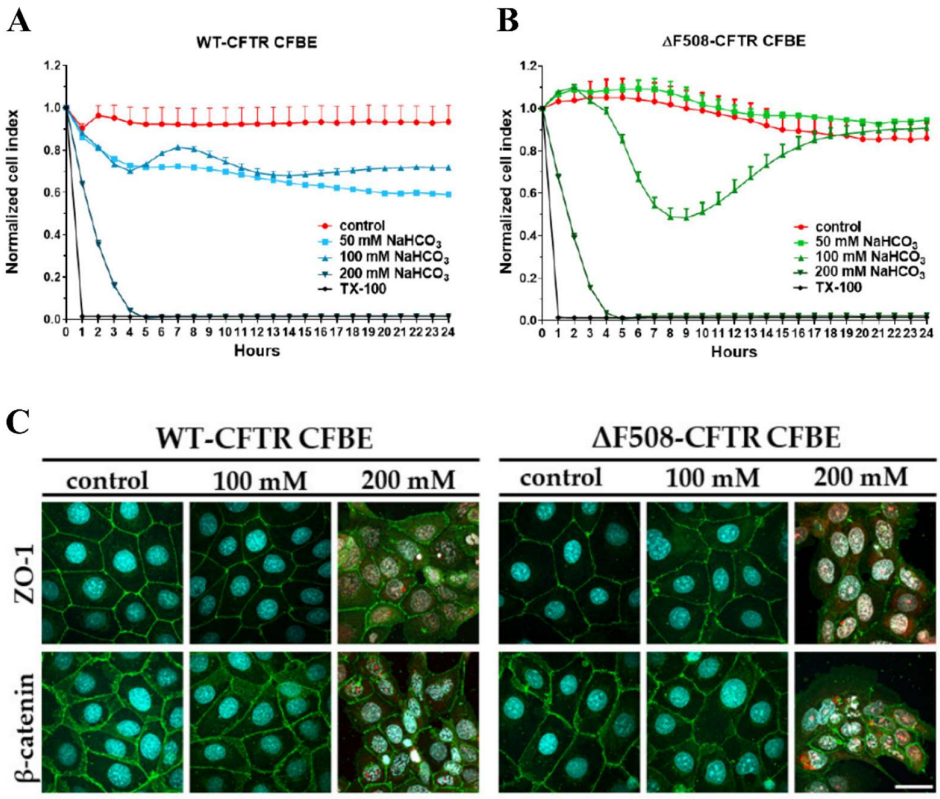

Figure 20. Airway epithelial cell tolerability testing after sodium bicarbonate treatment. Impedance kinetics measurements of the WT-CFTR CFBE **(A)** and ΔF508-CFTR CFBE **(B)** cells after sodium bicarbonate treatment at different concentrations (50, 100, 200 mM). **(C)** Morphology of CFBE cells after sodium bicarbonate treatment at different concentrations for 24 h. Green color: immunostaining for junctional proteins. Cyan color: cell nuclei. Red color: nuclei of damaged cells. Bar: 40 μm. The figure was reprinted from "The effect of sodium bicarbonate, a beneficial adjuvant molecule in cystic fibrosis, on bronchial epithelial cells expressing a wild-type or mutant CFTR channel" by Gróf, I. *et al.*, *Int J Mol Sci.* (2020) [126].

This evidence suggests the safety of using HCO_3^- (up to 100 mM), which supports that HCO_3^- could be a therapeutic tool for CF lung disease. However, we speculate that combination therapy (HCO_3^- treatment, CFTR modulators, and symptomatic therapies) may be the best approach to treat CF patients.

DOI:10.14753/SE.2022.2632

6. Conclusions

In this study, we successfully developed a suitable preparation procedure to prepare a unique medium (ASM) that resembles the CF airway environment to study the effects of HCO_3^- *per se* on CF bacteria.

HCO_3^- inhibits the growth of *S. aureus* and *P. aeruginosa*, the most prevalent CF bacteria. HCO_3^- also suppresses *P. aeruginosa* biofilm formation. Importantly, we detected these inhibitory effects in both conventional medium and ASM. The composition of the latter medium resembles the CF airway mucus, suggesting that the inhibitory effects of HCO_3^- might also exist in CF lung. We demonstrated that these effects are independent of changes in pH and osmolality, suggesting that the inhibitory effects are merely induced by HCO_3^- *per se*. We also showed that HCO_3^- effects were concentration-dependent.

Taken together, we demonstrated that HCO_3^- has antimicrobial effects. Furthermore, HCO_3^- restores airway pH, mucus secretion, and bacterial killing capacity. Since recent evidence has also suggested that HCO_3^- is safe on bronchial epithelial cells, inhalation of aerosolized HCO_3^- could be a potential symptomatic therapy for CF lung disease and other airway diseases (e.g., COPD) associated with mucus accumulation and bacterial infection.

DOI:10.14753/SE.2022.2632

7. Summary

Cystic fibrosis (CF) is a genetic disease caused by mutations in the gene encoding the CFTR channel. In CF, the mutations cause Cl^- and HCO_3^- hyposecretion, leading to airway dehydration, acidification, and viscous mucus production. This mucus is ideal for colonization by pathogenic bacteria. *P. aeruginosa* and *S. aureus* are the most common bacteria detected in the CF airways. These bacteria are frequently associated with biofilm-induced infections and progressive lung function decline due to repeated infections, inflammations, and tissue remodeling. This vicious cycle eventually leads to death due to pulmonary failure. HCO_3^- has shown its clinical importance in airway physiology. Not only does taking part in the extracellular fluid movement, but it also influences the airway pH buffering system, mucus homeostasis, and innate immune system. The antimicrobial effects of HCO_3^- have also been discussed. However, because of limited data, it is still unclear whether these effects are induced by HCO_3^- *per se,* its alkalinizing effects, or increased ionic strength. Here we demonstrate that the antimicrobial effects of HCO_3^- exist, and it is not due to an increase in pH or osmolality.

We tested the effects of 100 mM HCO_3^- on the growth of *P. aeruginosa* and *S. aureus* in brain-heart infusion (BHI) medium supplemented with 20% CO_2. The results showed that 100 mM HCO_3^- inhibited the growth of both bacteria. Since CF mucus is ideal for bacterial colonization, we also used an artificial sputum medium (ASM), a unique medium whose composition resembles CF mucus, to mimic the CF mucus. We developed a unique ASM that includes 25 or 100 mM $NaHCO_3$ to test its effects on bacterial growth and biofilm formation. The colony-forming unit assay and flow cytometry were used to count viable *P. aeruginosa* and *S. aureus* cells.

The data show that HCO_3^- significantly decreased viable cell counts and biofilm formation in a dose-dependent manner. These effects were due neither to extracellular alkalinization nor to altered osmolality. Our findings demonstrate that HCO_3^- exerts direct antibacterial and antibiofilm effects on prevalent CF bacteria. $NaHCO_3$ inhalation may be a practical therapeutic approach for CF and other infectious diseases in the airway.

DOI:10.14753/SE.2022.2632

8. Összefoglalás

A cisztás fibrózis (CF) egy öröklődő megbetegedés, amely a CFTR ioncsatornát kódoló génben létrejött mutáció miatt alakul ki. Cisztás fibrózisban a Cl^- és HCO_3^- ionok hiposzekréciója következik be, ami a légutakban lévő folyadékfilm volumenének és pH-jának csökkenéséhez, illetve sűrű nyákképződéshez vezet. Ez utóbbi ideális körülményeket teremt a patogén baktériumok kolonizációjához. A két leggyakoribb CF-ben szerepet játszó kórokozó a *P. aeruginosa* és a *S. aureus*. Ezek a baktériumok jellemzően biofilm képzők, és az általuk okozott sokszor visszatérő fertőzések és gyulladás progresszív tüdőfunkció romláshoz vezet. Ez az ördögi kör végül a tüdő teljes tönkremeneteléhez, következésképpen halálhoz vezethet. A HCO_3^- kiemelkedő klinikai jelentőséggel bír a légutak élettanában. Egyfelől szerepe van az elektrolit és folyadék kiválasztásban, másfelől befolyásolja a légúti pH-t, a mucus homeosztázist, sőt még a veleszületett immunrendszer működését is. Többen fölvetették a HCO_3^- antimikróbás hatását is. Azonban kevés adat áll rendelkezésre ezzel kapcsolatban, és nem világos, hogy maga a HCO_3^-, vagy esetleg az általa okozott erős lúgosodás és ionerősség áll-e a hatás hátterében. Jelen dolgozat eredményei igazolták, hogy a HCO_3^- valóban rendelkezik antibakteriális hatással és ez nem a pH vagy az ozmolalitás növekedésével függ össze.

Munkánk során teszteltük a 100 mM HCO_3^- hatását a *P. aeruginosa* és a *S. aureus* növekedésére 20% CO_2–vel equilibráltatott brain-heart infusion (BHI) táplevesben. Eredményeink világosan mutatják a 100 mM HCO_3^- baktérium-növekedést gátló hatását. Miután a CF-ben képződő sűrű nyák ideális közeg a bakteriális kolonizációhoz, egy ún. mesterséges köpetet (artificial sputum medium, ASM) is alkalmaztunk a kísérletekben, amely összetételében és tulajdonságaiban nagymértékben hasonlít a CF-ben keletkezett nyákra. Az eredeti ASM receptet továbbfejlesztettük úgy, hogy 25 vagy 100 mM $NaHCO_3$ tartalmú legyen, hogy ebben vizsgálhassuk a bikarbonát hatását a baktériumok növekedésre illetve a biofilm képzésre. Az élő *P. aeruginosa* és *S. aureus* sejtek mennyiségi meghatározására cfu mérést és áramlási citometriát használtunk.

Eredményeink azt mutatták, hogy a HCO_3^- koncentrációfüggő módon csökkentette az élő baktériumszámot, valamint a biofilmképzést. Kizártuk az extracelluláris lúgosodás, vagy a megváltozott ozmolalitás hatását. Kimondhatjuk tehát, hogy a HCO_3^- maga közvetlen antibakteriális és anti-biofilm hatással bír a két

DOI:10.14753/SE.2022.2632

legfontosabb CF kórokozó esetében. A $NaHCO_3$ inhalációnak ezért komoly terápiás szerepe lehet CF-ben, vagy egyéb fertőzéses eredetű légúti megbetegedésben.

9. Bibliography

1. Riordan, J.R.; Rommens, J.M.; Kerem, B.; Alon, N.; Rozmahel, R.; Grzelczak, Z.; Zielenski, J.; Lok, S.; Plavsic, N.; Chou, J.L.; *et al*. Identification of the cystic fibrosis gene: cloning and characterization of complementary DNA. *Science.* **1989**, *245*, 1066-1073, doi:10.1126/science.2475911.

2. Linsdell, P.; Tabcharani, J.A.; Rommens, J.M.; Hou, Y.X.; Chang, X.B.; Tsui, L.C.; Riordan, J.R.; Hanrahan, J.W. Permeability of wild-type and mutant cystic fibrosis transmembrane conductance regulator chloride channels to polyatomic anions. *J Gen Physiol.* **1997**, *110*, 355-364, doi:10.1085/jgp.110.4.355.

3. Reddy, M.M.; Quinton, P.M. Control of dynamic CFTR selectivity by glutamate and ATP in epithelial cells. *Nature.* **2003**, *423*, 756-760, doi:10.1038/nature01694.

4. Ballard, S.T.; Trout, L.; Bebök, Z.; Sorscher, E.J.; Crews, A. CFTR involvement in chloride, bicarbonate, and liquid secretion by airway submucosal glands. *Am J Physiol.* **1999**, *277*, L694-699, doi:10.1152/ajplung.1999.277.4.L694.

5. Livraghi-Butrico, A.; Kelly, E.J.; Wilkinson, K.J.; Rogers, T.D.; Gilmore, R.C.; Harkema, J.R.; Randell, S.H.; Boucher, R.C.; O'Neal, W.K.; Grubb, B.R. Loss of cftr function exacerbates the phenotype of Na(+) hyperabsorption in murine airways. *Am J Physiol Lung Cell Mol Physiol.* **2013**, *304*, L469-480, doi:10.1152/ajplung.00150.2012.

6. Kotnala, S.; Dhasmana, A.; Kashyap, V.K.; Chauhan, S.C.; Yallapu, M.M.; Jaggi, M. A bird eye view on cystic fibrosis: an underestimated multifaceted chronic disorder. *Life Sci.* **2021**, *268*, 118959, doi:10.1016/j.lfs.2020.118959.

7. Cystic Fibrosis Foundation [CFF]. *Patient registry: annual data report 2019*; 2019.

8. Cystic Fibrosis Canada [CFC]. *The Canadian cystic fibrosis registry: 2019 annual data report*; 2019.

9. Australian Cystic Fibrosis Data Registry [ACFDR]. *Australian cystic fibrosis data registry: annual report 2019*; 2019.

10. Brazilian Cystic Fibrosis Study Group [GBEFC]. *Registro brasileiro de fibrose cística 2018*; 2018.

11. European Cystic Fibrosis Society [ECFS]. *Patient registry: annual data report 2018*; 2018.

12. Burgel, P.R.; Bellis, G.; Olesen, H.V.; Viviani, L.; Zolin, A.; Blasi, F.; Elborn, J.S. Future trends in cystic fibrosis demography in 34 European countries. *Eur Respir J.* **2015**, *46*, 133-141, doi:10.1183/09031936.00196314.

13. Ahmed, S.; Cheok, G.; N-Goh, A.; Han, A.; Hong, S.; Indawati, W.; Lutful-Kabir, A.; Kabra, S.; Kamalaporn, H.; Kim, H.; Kunling, S.; Lochindarat, S.; Moslehi, M.; Nathan, A.; Ng, D.; The-Phung, N.; Singh, V.; Takase, M.; Triasih, R.; Dai, Z. Cystic fibrosis in Asia. *Pediatr Respir Crit Care Med.* **2020**, *4*, 8-12, doi:10.4103/prcm.prcm_5_20.

14. Busch, R. On the history of cystic fibrosis. *Acta Univ Carol Med (Praha).* **1990**, *36*, 13-15.

15. Blanchard, A.C.; Waters, V.J. Microbiology of cystic fibrosis airway disease. *Semin Respir Crit Care Med.* **2019**, *40*, 727-736, doi:10.1055/s-0039-1698464.

16. Rey, M.M.; Bonk, M.P.; Hadjiliadis, D. Cystic fibrosis: emerging understanding and therapies. *Annu Rev Med.* **2019**, *70*, 197-210, doi:10.1146/annurev-med-112717-094536.

17. Cystic Fibrosis Foundation [CFF]. *2019 Cystic fibrosis foundation patient registry highlights*; 2019.

18. Cystic Fibrosis Foundation [CFF]. *2016 Cystic fibrosis foundation patient registry highlights*; 2016.

19. Cystic Fibrosis Foundation [CFF]. *2017 Cystic fibrosis foundation patient registry highlights*; 2017.

20. Andersen, D.H. Cystic fibrosis of the pancreas and its relation to celiac disease: a clinical and pathologic study. *Am J Dis Child.* **1938**, *56*, 344-399, doi:10.1001/archpedi.1938.01980140114013.

21. Rommens, J.M.; Iannuzzi, M.C.; Kerem, B.; Drumm, M.L.; Melmer, G.; Dean, M.; Rozmahel, R.; Cole, J.L.; Kennedy, D.; Hidaka, N.; *et al*. Identification of the cystic fibrosis gene: chromosome walking and jumping. *Science.* **1989**, *245*, 1059-1065, doi:10.1126/science.2772657.

22. Kerem, B.; Rommens, J.M.; Buchanan, J.A.; Markiewicz, D.; Cox, T.K.; Chakravarti, A.; Buchwald, M.; Tsui, L.C. Identification of the cystic fibrosis gene: genetic analysis. *Science.* **1989**, *245*, 1073-1080, doi:10.1126/science.2570460.

23. Zhang, Z.; Liu, F.; Chen, J. Conformational changes of CFTR upon phosphorylation and ATP binding. *Cell.* **2017**, *170*, 483-491.e488, doi:10.1016/j.cell.2017.06.041.

24. Liu, F.; Zhang, Z.; Csanády, L.; Gadsby, D.C.; Chen, J. Molecular structure of the human CFTR ion channel. *Cell.* **2017**, *169*, 85-95.e88, doi:10.1016/j.cell.2017.02.024.

25. Lopes-Pacheco, M. CFTR modulators: shedding light on precision medicine for cystic fibrosis. *Front Pharmacol.* **2016**, *7*, 275, doi:10.3389/fphar.2016.00275.

26. Gadsby, D.C.; Vergani, P.; Csanády, L. The ABC protein turned chloride channel whose failure causes cystic fibrosis. *Nature.* **2006**, *440*, 477-483, doi:10.1038/nature04712.

27. Linsdell, P. Mechanism of chloride permeation in the cystic fibrosis transmembrane conductance regulator chloride channel. *Exp Physiol.* **2006**, *91*, 123-129, doi:10.1113/expphysiol.2005.031757.

28. Guggino, W.B.; Stanton, B.A. New insights into cystic fibrosis: molecular switches that regulate CFTR. *Nat Rev Mol Cell Biol.* **2006**, *7*, 426-436, doi:10.1038/nrm1949.

29. Bergeron, C.; Cantin, A.M. Cystic fibrosis: pathophysiology of lung disease. *Semin Respir Crit Care Med.* **2019**, *40*, 715-726, doi:10.1055/s-0039-1694021.

30. De Boeck, K.; Amaral, M.D. Progress in therapies for cystic fibrosis. *Lancet Respir Med.* **2016**, *4*, 662-674, doi:10.1016/s2213-2600(16)00023-0.

31. De Boeck, K. Cystic fibrosis in the year 2020: a disease with a new face. *Acta Paediatr.* **2020**, *109*, 893-899, doi:10.1111/apa.15155.

32. Bobadilla, J.L.; Macek, M., Jr.; Fine, J.P.; Farrell, P.M. Cystic fibrosis: a worldwide analysis of CFTR mutations - correlation with incidence data and application to screening. *Hum Mutat.* **2002**, *19*, 575-606, doi:10.1002/humu.10041.

33. Castellani, C.; Assael, B.M. Cystic fibrosis: a clinical view. *Cell Mol Life Sci.* **2017**, *74*, 129-140, doi:10.1007/s00018-016-2393-9.

34. Farinha, C.M.; Canato, S. From the endoplasmic reticulum to the plasma membrane: mechanisms of CFTR folding and trafficking. *Cell Mol Life Sci.* **2017**, *74*, 39-55, doi:10.1007/s00018-016-2387-7.

35. Tate, S.; MacGregor, G.; Davis, M.; Innes, J.A.; Greening, A.P. Airways in cystic fibrosis are acidified: detection by exhaled breath condensate. *Thorax.* **2002**, *57*, 926-929, doi:10.1136/thorax.57.11.926.

36. Stoltz, D.A.; Meyerholz, D.K.; Welsh, M.J. Origins of cystic fibrosis lung disease. *N Engl J Med.* **2015**, *372*, 351-362, doi:10.1056/NEJMra1300109.

37. Matsui, H.; Wagner, V.E.; Hill, D.B.; Schwab, U.E.; Rogers, T.D.; Button, B.; Taylor, R.M., 2nd; Superfine, R.; Rubinstein, M.; Iglewski, B.H.; Boucher, R.C. A physical linkage between cystic fibrosis airway surface dehydration and *Pseudomonas aeruginosa* biofilms. *Proc Natl Acad Sci U S A.* **2006**, *103*, 18131-18136, doi:10.1073/pnas.0606428103.

38. Simonin, J.; Bille, E.; Crambert, G.; Noel, S.; Dreano, E.; Edwards, A.; Hatton, A.; Pranke, I.; Villeret, B.; Cottart, C.H.; Vrel, J.P.; Urbach, V.; Baatallah, N.; Hinzpeter, A.; Golec, A.; Touqui, L.; Nassif, X.; Galietta, L.J.V.; Planelles, G.; Sallenave, J.M.; Edelman, A.; Sermet-Gaudelus, I. Airway surface liquid acidification initiates host defense abnormalities in cystic fibrosis. *Sci Rep.* **2019**, *9*, 6516, doi:10.1038/s41598-019-42751-4.

39. Ryu, J.H.; Kim, C.H.; Yoon, J.H. Innate immune responses of the airway epithelium. *Mol Cells.* **2010**, *30*, 173-183, doi:10.1007/s10059-010-0146-4.

40. Lyczak, J.B.; Cannon, C.L.; Pier, G.B. Lung infections associated with cystic fibrosis. *Clin Microbiol Rev.* **2002**, *15*, 194-222, doi:10.1128/cmr.15.2.194-222.2002.

41. McDaniel, C.; Panmanee, W.; Hassett, D.J. An overview of infections in cystic fibrosis airways and the role of environmental conditions on *Pseudomonas aeruginosa* biofilm formation and viability. In *Cystic Fibrosis in the Light of New Research*, Wat, D., Ed. IntechOpen: 2015; pp. 171-199.

42. Fothergill, J.L.; Neill, D.R.; Loman, N.; Winstanley, C.; Kadioglu, A. *Pseudomonas aeruginosa* adaptation in the nasopharyngeal reservoir leads to migration and persistence in the lungs. *Nat Commun.* **2014**, *5*, 4780, doi:10.1038/ncomms5780.

43. Rivas Caldas, R.; Le Gall, F.; Revert, K.; Rault, G.; Virmaux, M.; Gouriou, S.; Héry-Arnaud, G.; Barbier, G.; Boisramé, S. *Pseudomonas aeruginosa* and periodontal pathogens in the oral cavity and lungs of cystic fibrosis patients: a case-control study. *J Clin Microbiol.* **2015**, *53*, 1898-1907, doi:10.1128/jcm.00368-15.

44. Vieira Colombo, A.P.; Magalhães, C.B.; Hartenbach, F.A.; Martins do Souto, R.; Maciel da Silva-Boghossian, C. Periodontal-disease-associated biofilm: a reservoir for pathogens of medical importance. *Microb Pathog.* **2016**, *94*, 27-34, doi:10.1016/j.micpath.2015.09.009.

45. Heltshe, S.L.; Khan, U.; Beckett, V.; Baines, A.; Emerson, J.; Sanders, D.B.; Gibson, R.L.; Morgan, W.; Rosenfeld, M. Longitudinal development of initial, chronic and mucoid *Pseudomonas aeruginosa* infection in young children with cystic fibrosis. *J Cyst Fibros.* **2018**, *17*, 341-347, doi:10.1016/j.jcf.2017.10.008.

46. Kenna, D.T.; Doherty, C.J.; Foweraker, J.; Macaskill, L.; Barcus, V.A.; Govan, J.R.W. Hypermutability in environmental *Pseudomonas aeruginosa* and in populations causing pulmonary infection in individuals with cystic fibrosis. *Microbiology (Reading).* **2007**, *153*, 1852-1859, doi:10.1099/mic.0.2006/005082-0.

47. Madsen, J.S.; Burmølle, M.; Hansen, L.H.; Sørensen, S.J. The interconnection between biofilm formation and horizontal gene transfer. *FEMS Immunol Med Microbiol.* **2012**, *65*, 183-195, doi:10.1111/j.1574-695X.2012.00960.x.

48. Ghigo, J.M. Natural conjugative plasmids induce bacterial biofilm development. *Nature.* **2001**, *412*, 442-445, doi:10.1038/35086581.

49. Lerminiaux, N.A.; Cameron, A.D.S. Horizontal transfer of antibiotic resistance genes in clinical environments. *Can J Microbiol.* **2019**, *65*, 34-44, doi:10.1139/cjm-2018-0275.

50. Mastella, G.; Rainisio, M.; Harms, H.K.; Hodson, M.E.; Koch, C.; Navarro, J.; Strandvik, B.; McKenzie, S.G. Allergic bronchopulmonary aspergillosis in cystic fibrosis. A European epidemiological study. Epidemiologic Registry of Cystic Fibrosis. *Eur Respir J.* **2000**, *16*, 464-471, doi:10.1034/j.1399-3003.2000.016003464.x.

51. Tré-Hardy, M.; Macé, C.; El Manssouri, N.; Vanderbist, F.; Traore, H.; Devleeschouwer, M.J. Effect of antibiotic co-administration on young and mature biofilms of cystic fibrosis clinical isolates: the importance of the biofilm model. *Int J Antimicrob Agents.* **2009**, *33*, 40-45, doi:10.1016/j.ijantimicag.2008.07.012.

52. Song, Y.; Thiagarajah, J.; Verkman, A.S. Sodium and chloride concentrations, pH, and depth of airway surface liquid in distal airways. *J Gen Physiol.* **2003**, *122*, 511-519, doi:10.1085/jgp.200308866.

53. Widdicombe, J.H. Regulation of the depth and composition of airway surface liquid. *J Anat.* **2002**, *201*, 313-318, doi:10.1046/j.1469-7580.2002.00098.x.

54. Shei, R.J.; Peabody, J.E.; Rowe, S.M. Functional Anatomic Imaging of the Airway Surface. *Ann Am Thorac Soc.* **2018**, *15*, S177-183, doi:10.1513/AnnalsATS.201806-407AW.

55. Haq, I.J.; Gray, M.A.; Garnett, J.P.; Ward, C.; Brodlie, M. Airway surface liquid homeostasis in cystic fibrosis: pathophysiology and therapeutic targets. *Thorax.* **2016**, *71*, 284-287, doi:10.1136/thoraxjnl-2015-207588.

56. Button, B.; Cai, L.H.; Ehre, C.; Kesimer, M.; Hill, D.B.; Sheehan, J.K.; Boucher, R.C.; Rubinstein, M. A periciliary brush promotes the lung health by separating

the mucus layer from airway epithelia. *Science.* **2012**, *337*, 937-941, doi:10.1126/science.1223012.

57. Widdicombe, J.G. Airway surface liquid: concepts and measurements. In *Airway Mucus: Basic Mechanisms and Clinical Perspectives*, Rogers, D.F., Lethem, M.I., Eds. Birkhäuser Basel: Basel, 1997; pp. 1-17.

58. Robinson, N.P.; Kyle, H.; Webber, S.E.; Widdicombe, J.G. Electrolyte and other chemical concentrations in tracheal airway surface liquid and mucus. *J Appl Physiol (1985).* **1989**, *66*, 2129-2135, doi:10.1152/jappl.1989.66.5.2129.

59. Widdicombe, J.H.; Widdicombe, J.G. Regulation of human airway surface liquid. *Respir Physiol.* **1995**, *99*, 3-12, doi:10.1016/0034-5687(94)00095-h.

60. Boucher, R.C. Regulation of airway surface liquid volume by human airway epithelia. *Pflügers Archiv.* **2003**, *445*, 495-498, doi:10.1007/s00424-002-0955-1.

61. Evans, C.M.; Koo, J.S. Airway mucus: the good, the bad, the sticky. *Pharmacol Ther.* **2009**, *121*, 332-348, doi:10.1016/j.pharmthera.2008.11.001.

62. Borowitz, D. CFTR, bicarbonate, and the pathophysiology of cystic fibrosis. *Pediatr Pulmonol.* **2015**, *50 Suppl 40*, S24-30, doi:10.1002/ppul.23247.

63. Quinton, P.M. Cystic fibrosis: impaired bicarbonate secretion and mucoviscidosis. *Lancet.* **2008**, *372*, 415-417, doi:10.1016/s0140-6736(08)61162-9.

64. Ermund, A.; Trillo-Muyo, S.; Hansson, G.C. Assembly, release, and transport of airway mucins in pigs and humans. *Ann Am Thorac Soc.* **2018**, *15*, S159-163, doi:10.1513/AnnalsATS.201804-238AW.

65. Zajac, M.; Dreano, E.; Edwards, A.; Planelles, G.; Sermet-Gaudelus, I. Airway surface liquid pH regulation in airway epithelium current understandings and gaps in knowledge. *Int J Mol Sci.* **2021**, *22*, doi:10.3390/ijms22073384.

66. McShane, D.; Davies, J.C.; Davies, M.G.; Bush, A.; Geddes, D.M.; Alton, E.W. Airway surface pH in subjects with cystic fibrosis. *Eur Respir J.* **2003**, *21*, 37-42, doi:10.1183/09031936.03.00027603.

67. Kim, D.; Liao, J.; Hanrahan, J.W. The buffer capacity of airway epithelial secretions. *Front Physiol.* **2014**, *5*, 188, doi:10.3389/fphys.2014.00188.

68. Hiemstra, P.S.; McCray, P.B., Jr.; Bals, R. The innate immune function of airway epithelial cells in inflammatory lung disease. *Eur Respir J.* **2015**, *45*, 1150-1162, doi:10.1183/09031936.00141514.

69. Birket, S.E.; Chu, K.K.; Liu, L.; Houser, G.H.; Diephuis, B.J.; Wilsterman, E.J.; Dierksen, G.; Mazur, M.; Shastry, S.; Li, Y.; Watson, J.D.; Smith, A.T.; Schuster, B.S.; Hanes, J.; Grizzle, W.E.; Sorscher, E.J.; Tearney, G.J.; Rowe, S.M. A functional anatomic defect of the cystic fibrosis airway. *Am J Respir Crit Care Med.* **2014**, *190*, 421-432, doi:10.1164/rccm.201404-0670OC.

70. Brogden, K.A. Antimicrobial peptides: pore formers or metabolic inhibitors in bacteria? *Nat Rev Microbiol.* **2005**, *3*, 238-250, doi:10.1038/nrmicro1098.

71. Zarzosa-Moreno, D.; Avalos-Gómez, C.; Ramírez-Texcalco, L.S.; Torres-López, E.; Ramírez-Mondragón, R.; Hernández-Ramírez, J.O.; Serrano-Luna, J.; de la Garza, M. Lactoferrin and Its Derived Peptides: An Alternative for Combating Virulence Mechanisms Developed by Pathogens. *Molecules.* **2020**, *25*, doi:10.3390/molecules25245763.

72. Pezzulo, A.A.; Tang, X.X.; Hoegger, M.J.; Abou Alaiwa, M.H.; Ramachandran, S.; Moninger, T.O.; Karp, P.H.; Wohlford-Lenane, C.L.; Haagsman, H.P.; van Eijk, M.; Bánfi, B.; Horswill, A.R.; Stoltz, D.A.; McCray, P.B., Jr.; Welsh, M.J.; Zabner, J. Reduced airway surface pH impairs bacterial killing in the porcine cystic fibrosis lung. *Nature.* **2012**, *487*, 109-113, doi:10.1038/nature11130.

73. Dorschner, R.A.; Lopez-Garcia, B.; Peschel, A.; Kraus, D.; Morikawa, K.; Nizet, V.; Gallo, R.L. The mammalian ionic environment dictates microbial susceptibility to antimicrobial defense peptides. *FASEB J.* **2006**, *20*, 35-42, doi:10.1096/fj.05-4406com.

74. Oliveira, A.S.; Vaz, C.V.; Silva, A.; Ferreira, S.S.; Correia, S.; Ferreira, R.; Breitenfeld, L.; Martinez-de-Oliveira, J.; Palmeira-de-Oliveira, R.; Pereira, C.; Cruz, M.T.; Palmeira-de-Oliveira, A. Chemical signature and antimicrobial activity of central Portuguese natural mineral waters against selected skin

pathogens. *Environ Geochem Health.* **2020**, *42*, 2039-2057, doi:10.1007/s10653-019-00473-6.

75. Rutala, W.A.; Barbee, S.L.; Aguiar, N.C.; Sobsey, M.D.; Weber, D.J. Antimicrobial activity of home disinfectants and natural products against potential human pathogens. *Infect Control Hosp Epidemiol.* **2000**, *21*, 33-38, doi:10.1086/501694.

76. Corral, L.G.; Post, L.S.; Montville, T.J. Antimicrobial activity of sodium bicarbonate. *J Food Sci.* **1988**, *53*, 981-982, doi:10.1111/j.1365-2621.1988.tb09005.x.

77. Madeswaran, S.; Jayachandran, S. Sodium bicarbonate: a review and its uses in dentistry. *Indian J Dent Res.* **2018**, *29*, 672-677, doi:10.4103/ijdr.IJDR_30_17.

78. Lagier, J.C.; Edouard, S.; Pagnier, I.; Mediannikov, O.; Drancourt, M.; Raoult, D. Current and past strategies for bacterial culture in clinical microbiology. *Clin Microbiol Rev.* **2015**, *28*, 208-236, doi:10.1128/cmr.00110-14.

79. Ghani, M.; Soothill, J.S. Ceftazidime, gentamicin, and rifampicin, in combination, kill biofilms of mucoid *Pseudomonas aeruginosa*. *Can J Microbiol.* **1997**, *43*, 999-1004, doi:10.1139/m97-144.

80. Sriramulu, D.D.; Lünsdorf, H.; Lam, J.S.; Römling, U. Microcolony formation: a novel biofilm model of *Pseudomonas aeruginosa* for the cystic fibrosis lung. *J Med Microbiol.* **2005**, *54*, 667-676, doi:10.1099/jmm.0.45969-0.

81. Palmer, K.L.; Aye, L.M.; Whiteley, M. Nutritional cues control *Pseudomonas aeruginosa* multicellular behavior in cystic fibrosis sputum. *J Bacteriol.* **2007**, *189*, 8079-8087, doi:10.1128/jb.01138-07.

82. Fung, C.; Naughton, S.; Turnbull, L.; Tingpej, P.; Rose, B.; Arthur, J.; Hu, H.; Harmer, C.; Harbour, C.; Hassett, D.J.; Whitchurch, C.B.; Manos, J. Gene expression of *Pseudomonas aeruginosa* in a mucin-containing synthetic growth medium mimicking cystic fibrosis lung sputum. *J Med Microbiol.* **2010**, *59*, 1089-1100, doi:10.1099/jmm.0.019984-0.

83. Sriramulu, D.D. Artificial sputum medium. In *Protoc Exch*, 2010.

84. Kirchner, S.; Fothergill, J.L.; Wright, E.A.; James, C.E.; Mowat, E.; Winstanley, C. Use of artificial sputum medium to test antibiotic efficacy against *Pseudomonas aeruginosa* in conditions more relevant to the cystic fibrosis lung. *J Vis Exp.* **2012**, e3857, doi:10.3791/3857.

85. Yeung, A.T.; Parayno, A.; Hancock, R.E. Mucin promotes rapid surface motility in *Pseudomonas aeruginosa*. *mBio.* **2012**, *3*, e00073-00012, doi:10.1128/mBio.00073-12.

86. Behrends, V.; Geier, B.; Williams, H.D.; Bundy, J.G. Direct assessment of metabolite utilization by *Pseudomonas aeruginosa* during growth on artificial sputum medium. *Appl Environ Microbiol.* **2013**, *79*, 2467-2470, doi:10.1128/aem.03609-12.

87. Wright, E.A.; Fothergill, J.L.; Paterson, S.; Brockhurst, M.A.; Winstanley, C. Sub-inhibitory concentrations of some antibiotics can drive diversification of *Pseudomonas aeruginosa* populations in artificial sputum medium. *BMC Microbiol.* **2013**, *13*, 170, doi:10.1186/1471-2180-13-170.

88. Quinn, R.A.; Whiteson, K.; Lim, Y.W.; Salamon, P.; Bailey, B.; Mienardi, S.; Sanchez, S.E.; Blake, D.; Conrad, D.; Rohwer, F. A Winogradsky-based culture system shows an association between microbial fermentation and cystic fibrosis exacerbation. *Isme j.* **2015**, *9*, 1024-1038, doi:10.1038/ismej.2014.234.

89. Davies, E.V.; James, C.E.; Brockhurst, M.A.; Winstanley, C. Evolutionary diversification of *Pseudomonas aeruginosa* in an artificial sputum model. *BMC Microbiol.* **2017**, *17*, 3, doi:10.1186/s12866-016-0916-z.

90. Haley, C.L.; Colmer-Hamood, J.A.; Hamood, A.N. Characterization of biofilm-like structures formed by *Pseudomonas aeruginosa* in a synthetic mucus medium. *BMC Microbiol.* **2012**, *12*, 181, doi:10.1186/1471-2180-12-181.

91. Sieuwerts, S.; de Bok, F.A.; Mols, E.; de vos, W.M.; Vlieg, J.E. A simple and fast method for determining colony forming units. *Lett Appl Microbiol.* **2008**, *47*, 275-278, doi:10.1111/j.1472-765X.2008.02417.x.

92. Grégori, G.; Citterio, S.; Ghiani, A.; Labra, M.; Sgorbati, S.; Brown, S.; Denis, M. Resolution of viable and membrane-compromised bacteria in freshwater and

marine waters based on analytical flow cytometry and nucleic acid double staining. *Appl Environ Microbiol.* **2001**, *67*, 4662-4670, doi:10.1128/aem.67.10.4662-4670.2001.

93. Robertson, J.; McGoverin, C.; Vanholsbeeck, F.; Swift, S. Optimisation of the Protocol for the LIVE/DEAD(®) BacLight(TM) Bacterial Viability Kit for Rapid Determination of Bacterial Load. *Front Microbiol.* **2019**, *10*, 801, doi:10.3389/fmicb.2019.00801.

94. Stiefel, P.; Schmidt-Emrich, S.; Maniura-Weber, K.; Ren, Q. Critical aspects of using bacterial cell viability assays with the fluorophores SYTO9 and propidium iodide. *BMC Microbiol.* **2015**, *15*, 36, doi:10.1186/s12866-015-0376-x.

95. O'Toole, G.; Kaplan, H.B.; Kolter, R. Biofilm formation as microbial development. *Annu Rev Microbiol.* **2000**, *54*, 49-79, doi:10.1146/annurev.micro.54.1.49.

96. Burton, E.; Yakandawala, N.; LoVetri, K.; Madhyastha, M.S. A microplate spectrofluorometric assay for bacterial biofilms. *J Ind Microbiol Biotechnol.* **2007**, *34*, 1-4, doi:10.1007/s10295-006-0086-3.

97. Huynh, T.T.; McDougald, D.; Klebensberger, J.; Al Qarni, B.; Barraud, N.; Rice, S.A.; Kjelleberg, S.; Schleheck, D. Glucose starvation-induced dispersal of *Pseudomonas aeruginosa* biofilms is cAMP and energy dependent. *PLoS One.* **2012**, *7*, e42874, doi:10.1371/journal.pone.0042874.

98. Comstock, W.J.; Huh, E.; Weekes, R.; Watson, C.; Xu, T.; Dorrestein, P.C.; Quinn, R.A. The winCF model - an inexpensive and tractable microcosm of a mucus plugged bronchiole to study the microbiology of lung infections. *J Vis Exp.* **2017**, doi:10.3791/55532.

99. Stites, S.W.; Walters, B.; O'Brien-Ladner, A.R.; Bailey, K.; Wesselius, L.J. Increased iron and ferritin content of sputum from patients with cystic fibrosis or chronic bronchitis. *Chest.* **1998**, *114*, 814-819, doi:10.1378/chest.114.3.814.

100. Rogan, M.P.; Taggart, C.C.; Greene, C.M.; Murphy, P.G.; O'Neill, S.J.; McElvaney, N.G. Loss of microbicidal activity and increased formation of biofilm

due to decreased lactoferrin activity in patients with cystic fibrosis. *J Infect Dis.* **2004**, *190*, 1245-1253, doi:10.1086/423821.

101. Reid, D.W.; Withers, N.J.; Francis, L.; Wilson, J.W.; Kotsimbos, T.C. Iron deficiency in cystic fibrosis: relationship to lung disease severity and chronic *Pseudomonas aeruginosa* infection. *Chest.* **2002**, *121*, 48-54, doi:10.1378/chest.121.1.48.

102. Dobay, O.; Laub, K.; Stercz, B.; Kéri, A.; Balázs, B.; Tóthpál, A.; Kardos, S.; Jaikumpun, P.; Ruksakiet, K.; Quinton, P.M.; Zsembery, Á. Bicarbonate inhibits bacterial growth and biofilm formation of prevalent cystic fibrosis pathogens. *Front Microbiol.* **2018**, *9*, 2245, doi:10.3389/fmicb.2018.02245.

103. Horváth, A.; Dobay, O.; Kardos, S.; Ghidán, Á.; Tóth, Á.; Pászti, J.; Ungvári, E.; Horváth, P.; Nagy, K.; Zissman, S.; Füzi, M. Varying fitness cost associated with resistance to fluoroquinolones governs clonal dynamic of methicillin-resistant *Staphylococcus aureus*. *Eur J Clin Microbiol Infect Dis.* **2012**, *31*, 2029-2036, doi:10.1007/s10096-011-1536-z.

104. Berney, M.; Hammes, F.; Bosshard, F.; Weilenmann, H.U.; Egli, T. Assessment and interpretation of bacterial viability by using the LIVE/DEAD BacLight Kit in combination with flow cytometry. *Appl Environ Microbiol.* **2007**, *73*, 3283-3290, doi:10.1128/aem.02750-06.

105. Gustafsson, J.K.; Ermund, A.; Ambort, D.; Johansson, M.E.; Nilsson, H.E.; Thorell, K.; Hebert, H.; Sjövall, H.; Hansson, G.C. Bicarbonate and functional CFTR channel are required for proper mucin secretion and link cystic fibrosis with its mucus phenotype. *J Exp Med.* **2012**, *209*, 1263-1272, doi:10.1084/jem.20120562.

106. Farha, M.A.; French, S.; Stokes, J.M.; Brown, E.D. Bicarbonate alters bacterial susceptibility to antibiotics by targeting the proton motive Force. *ACS Infect Dis.* **2018**, *4*, 382-390, doi:10.1021/acsinfecdis.7b00194.

107. Xie, C.; Tang, X.; Xu, W.; Diao, R.; Cai, Z.; Chan, H.C. A host defense mechanism involving CFTR-mediated bicarbonate secretion in bacterial prostatitis. *PLoS One.* **2010**, *5*, e15255, doi:10.1371/journal.pone.0015255.

108. Hoefel, D.; Grooby, W.L.; Monis, P.T.; Andrews, S.; Saint, C.P. Enumeration of water-borne bacteria using viability assays and flow cytometry: a comparison to culture-based techniques. *J Microbiol Methods.* **2003**, *55*, 585-597, doi:10.1016/s0167-7012(03)00201-x.

109. Hu, W.; Murata, K.; Zhang, D. Applicability of LIVE/DEAD BacLight stain with glutaraldehyde fixation for the measurement of bacterial abundance and viability in rainwater. *J Environ Sci (China).* **2017**, *51*, 202-213, doi:10.1016/j.jes.2016.05.030.

110. Thomas, K.J., 3rd; Rice, C.V. Revised model of calcium and magnesium binding to the bacterial cell wall. *Biometals.* **2014**, *27*, 1361-1370, doi:10.1007/s10534-014-9797-5.

111. Clifton, L.A.; Skoda, M.W.; Le Brun, A.P.; Ciesielski, F.; Kuzmenko, I.; Holt, S.A.; Lakey, J.H. Effect of divalent cation removal on the structure of Gram-negative bacterial outer membrane models. *Langmuir.* **2015**, *31*, 404-412, doi:10.1021/la504407v.

112. Walsh, S.E.; Maillard, J.Y.; Russell, A.D.; Catrenich, C.E.; Charbonneau, D.L.; Bartolo, R.G. Activity and mechanisms of action of selected biocidal agents on Gram-positive and -negative bacteria. *J Appl Microbiol.* **2003**, *94*, 240-247, doi:10.1046/j.1365-2672.2003.01825.x.

113. Sharma, M.; Visai, L.; Bragheri, F.; Cristiani, I.; Gupta, P.K.; Speziale, P. Toluidine blue-mediated photodynamic effects on staphylococcal biofilms. *Antimicrob Agents Chemother.* **2008**, *52*, 299-305, doi:10.1128/aac.00988-07.

114. Finnegan, S.; Percival, S.L. EDTA: an antimicrobial and antibiofilm agent for use in wound care. *Adv Wound Care (New Rochelle).* **2015**, *4*, 415-421, doi:10.1089/wound.2014.0577.

115. Alakomi, H.L.; Paananen, A.; Suihko, M.L.; Helander, I.M.; Saarela, M. Weakening effect of cell permeabilizers on Gram-negative bacteria causing biodeterioration. *Appl Environ Microbiol.* **2006**, *72*, 4695-4703, doi:10.1128/aem.00142-06.

116. Gawande, P.V.; LoVetri, K.; Yakandawala, N.; Romeo, T.; Zhanel, G.G.; Cvitkovitch, D.G.; Madhyastha, S. Antibiofilm activity of sodium bicarbonate, sodium metaperiodate and SDS combination against dental unit waterline-associated bacteria and yeast. *J Appl Microbiol.* **2008**, *105*, 986-992, doi:10.1111/j.1365-2672.2008.03823.x.

117. Pratten, J.; Wiecek, J.; Mordan, N.; Lomax, A.; Patel, N.; Spratt, D.; Middleton, A.M. Physical disruption of oral biofilms by sodium bicarbonate: an *in vitro* study. *Int J Dent Hyg.* **2016**, *14*, 209-214, doi:10.1111/idh.12162.

118. Rasamiravaka, T.; Randrianierenana, A.L.; Raherimamdimby, M.; Andrianarisoa, B. Effect of pH on biofilm formation and motilities of *Pseudomonas aeruginosa*, *Escherichia coli* and *Staphylococcus aureus* ATCC strains. *BMR Microbiology.* **2018**, *4*, 1-5.

119. Hostacká, A.; Ciznár, I.; Stefkovicová, M. Temperature and pH affect the production of bacterial biofilm. *Folia Microbiol (Praha).* **2010**, *55*, 75-78, doi:10.1007/s12223-010-0012-y.

120. Ramsey, B.W.; Davies, J.; McElvaney, N.G.; Tullis, E.; Bell, S.C.; Dřevínek, P.; Griese, M.; McKone, E.F.; Wainwright, C.E.; Konstan, M.W.; Moss, R.; Ratjen, F.; Sermet-Gaudelus, I.; Rowe, S.M.; Dong, Q.; Rodriguez, S.; Yen, K.; Ordoñez, C.; Elborn, J.S. A CFTR potentiator in patients with cystic fibrosis and the G551D mutation. *N Engl J Med.* **2011**, *365*, 1663-1672, doi:10.1056/NEJMoa1105185.

121. Sherrard, L.J.; Tunney, M.M.; Elborn, J.S. Antimicrobial resistance in the respiratory microbiota of people with cystic fibrosis. *Lancet.* **2014**, *384*, 703-713, doi:10.1016/s0140-6736(14)61137-5.

122. Kis, A.; Toth, L.A.; Kunos, L.; Vasas, S.; Losonczy, G.; Mendes, E.; Wanner, A.; Horvath, G. The effect of airway alkalization by nebulized sodium bicarbonate on airway blood flow. *European Respiratory Journal.* **2012**, *40*, P2143.

123. Birket, S.E.; Davis, J.M.; Fernandez, C.M.; Tuggle, K.L.; Oden, A.M.; Chu, K.K.; Tearney, G.J.; Fanucchi, M.V.; Sorscher, E.J.; Rowe, S.M. Development of an airway mucus defect in the cystic fibrosis rat. *JCI Insight.* **2018**, *3*, e97199, doi:10.1172/jci.insight.97199.

124. Garcia, M.A.; Yang, N.; Quinton, P.M. Normal mouse intestinal mucus release requires cystic fibrosis transmembrane regulator-dependent bicarbonate secretion. *J Clin Invest.* **2009**, *119*, 2613-2622, doi:10.1172/jci38662.

125. Gomez, C.C.S.; Parazzi, P.L.F.; Clinckspoor, K.J.; Mauch, R.M.; Pessine, F.B.T.; Levy, C.E.; Peixoto, A.O.; Ribeiro MÂ, G.O.; Ribeiro, A.F.; Conrad, D.; Quinton, P.M.; Marson, F.A.L.; Ribeiro, J.D. Safety, tolerability, and effects of sodium bicarbonate inhalation in cystic fibrosis. *Clin Drug Investig.* **2020**, *40*, 105-117, doi:10.1007/s40261-019-00861-x.

126. Gróf, I.; Bocsik, A.; Harazin, A.; Santa-Maria, A.R.; Vizsnyiczai, G.; Barna, L.; Kiss, L.; Fűr, G.; Rakonczay, Z., Jr.; Ambrus, R.; Szabó-Révész, P.; Gosselet, F.; Jaikumpun, P.; Szabó, H.; Zsembery, Á.; Deli, M.A. The effect of sodium bicarbonate, a beneficial adjuvant molecule in cystic fibrosis, on bronchial epithelial cells expressing a wild-type or mutant CFTR channel. *Int J Mol Sci.* **2020**, *21*, 4024, doi:10.3390/ijms21114024.

DOI:10.14753/SE.2022.2632

10. List of Own Publications

Original publications within the topic of the Ph.D. thesis:

1. Dobay, O., Laub, K., Stercz, B., Kéri, A., Balázs, B., Tóthpál, A., Kardos, S., **Jaikumpun, P.**, Ruksakiet, K., Quinton, P.M., and Zsembery, Á. (2018). Bicarbonate Inhibits Bacterial Growth and Biofilm Formation of Prevalent Cystic Fibrosis Pathogens. *Front Microbiol.* 9, 2245.
   Journal Article/Article (Journal Article)/Scientific
   SJR Scopus - Microbiology (medical): Q1
   IF: 4.259

2. Gróf, I., Bocsik, A., Harazin, A., Santa-Maria, A.R., Vizsnyiczai, G., Barna, L., Kiss, L., Fűr, G., Rakonczay, Z., Jr., Ambrus, R., Szabó-Révész, P., Gosselet, F., **Jaikumpun, P.**, Szabó, H., Zsembery, Á., and Deli, M.A. (2020). The Effect of Sodium Bicarbonate, a Beneficial Adjuvant Molecule in Cystic Fibrosis, on Bronchial Epithelial Cells Expressing a Wild-Type or Mutant CFTR Channel. *Int J Mol Sci.* 21, 4024.
   Journal Article/Article (Journal Article)/Scientific
   IF: 5.923

3. **Jaikumpun, P.**, Ruksakiet, K., Stercz, B., Pállinger, É., Steward, M., Lohinai, Z., Dobay, O., and Zsembery, Á. (2020). Antibacterial Effects of Bicarbonate in Media Modified to Mimic Cystic Fibrosis Sputum. *Int J Mol Sci.* 21.
   Journal Article/Article (Journal Article)/Scientific
   IF: 5.923

4. Ruksakiet, K., Stercz, B., Tóth, G., **Jaikumpun, P.**, Gróf, I., Tengölics, R., Lohinai, Z.M., Horváth, P., Deli, M.A., Steward, M.C., Dobay, O., and Zsembery, Á. (2021). Bicarbonate Evokes Reciprocal Changes in Intracellular Cyclic di-GMP and Cyclic AMP Levels in *Pseudomonas aeruginosa*. *Biology.* 10, 519.
   Journal Article/Article (Journal Article)/Scientific
   SJR Scopus - Agricultural and Biological Sciences (miscellaneous): D1
   IF: 5.079

5. Budai-Szűcs, M., Berkó, S., Kovács, A., Jaikumpun, P., Ambrus, R., Halász, A., Szabó-Révész, P., Csányi, E., and Zsembery, Á. (2021). Rheological effects of hypertonic saline and sodium bicarbonate solutions on cystic fibrosis sputum *in vitro*. BMC Pulm Med. 21, 225.
   IF: 4.1

Review (opinion) article not relating to the topic of the Ph.D. thesis:

1. Zsembery, Á., Kádár, K., **Jaikumpun, P.**, Deli, M., Jakab, F., and Dobay, O. Bicarbonate: An Ancient Concept to Defeat Pathogens in Light of Recent Findings Beneficial for COVID-19 Patients, (April 26, 2020). Available at SSRN: https://ssrn.com/abstract=3589403

DOI:10.14753/SE.2022.2632

11. Acknowledgment

I would like to thank my supervisors, Dr. Ákos Zsembery and Dr. Orsolya Dobay, for their professional and visionary supervision and extraordinary performance as my supervisors and advisors. They both are my role model not only for my academic career but also for my personal life.

I would also like to thank all members of my research team; Dr. Zsolt Lohinai, Dr. Éva Pállinger, Dr. Martin Steward, Balázs Stercz, and Dr. Kasidid Ruksakiet, for their advice and supervision. I also want to thank Dr. Anna Földes for her exceptional critique of my dissertation.

I want to give special thanks to Dr. Gábor Gerber and Prof. Dr. Gábor Varga, who initiated the program and brought Thai students here in Hungary.

Lastly, I would like to thank everyone in the Department of Oral Biology, Semmelweis University, as well as my family, colleagues, and friends in Hungary, Thailand, and the USA who always support me.